

**ISTANBUL TECHNICAL UNIVERSITY ★ GRADUATE SCHOOL OF SCIENCE**  
**ENGINEERING AND TECHNOLOGY**

**CONTROLLED RELEASE OF TETRACYCLINE HYDROCHLORIDE FROM  
COPOLYMER/GELATIN NANOFIBERS**



**M.Sc. THESIS**

**Ayşe METİN**

**Department of Polymer Science and Technology**

**Polymer Science and Technology**

**JULY, 2020**



**ISTANBUL TECHNICAL UNIVERSITY ★ GRADUATE SCHOOL OF SCIENCE**  
**ENGINEERING AND TECHNOLOGY**

**CONTROLLED RELEASE OF TETRACYCLINE HYDROCHLORIDE FROM  
COPOLYMER/GELATIN NANOFIBERS**

**M.Sc. THESIS**

**Ayşe METİN  
(515161027)**

**Department of Polymer Science and Technology**

**Polymer Science and Technology  
Programme**

**Thesis Advisor: Prof. Dr. Yüksel AVCIBAŞI GÜVENİLİR**

**JULY, 2020**



**İSTANBUL TEKNİK ÜNİVERSİTESİ ★ FEN BİLİMLERİ ENSTİTÜSÜ**

**KOPOLİMER/JELATİN NANOLİFLERİNDEN TETRASİKLİN  
HİDROKLORÜRÜN KONTROLLÜ SALINIMI**

**YÜKSEK LİSANS TEZİ**

**Ayşe METİN  
(515161027)**

**Polimer Bilimi ve Teknolojisi Ana Bilim Dalı**

**Polimer Bilimi ve Teknolojisi Programı**

**Tez Danışmanı: Prof. Dr. Yüksel AVCIBAŞI GÜVENİLİR**

**JULY, 2020**



Ayşe Metin, a M.Sc. student of İTÜ Graduate School of Science Engineering and Technology student 515161027, successfully defended the thesis entitled “CONTROLLED RELEASE OF TETRACYCLINE HYDROCHLORIDE FROM COPOLYMER/GELATIN NANOFIBERS”, which she prepared after fulfilling the requirements specified in the associated legislations, before the jury whose signatures are below.

**Thesis Advisor :**     **Prof. Dr. Yüksel AVCIBAŞI GÜVENİLİR** .....  
İstanbul Technical University

**Jury Members :**     **Prof. Dr. Ayşen ÖNEN** .....  
İstanbul Technical University

**Prof. Dr. Yaşar Andelib AYDIN** .....  
Marmara University

**Date of Submission : 30 June 2020**

**Date of Defense : 16 July 2020**





*To my family,*



## FOREWORD

First of all, I would like to thank my thesis advisor Prof Dr. Yüksel Avcıbaşı Güvenilir who supported me throughout this journey with her extensive knowledge and experience. I will always be grateful for her guidance and positive attitude during my education and dissertation preparations.

I would like to also convey my sincere gratitude for my dear lab partner Research Assistant Cansu Ülker Turan who guided me during my lab trials as well as academic research tasks. I wish her the best for her PhD dissertation and further academic journey. Furthermore, I would also like to thank Yasemin Kaptan for her great lab friendship and wish her the best on her academic studies.

On the other hand, I would like to convey my infinite gratitude to Asst. Prof. Dr. Yaşar Andelib Aydın for sharing her vast knowledge on Microbiology in order to contribute to my lab trials on antibacterial tests. I also thank Chemical Engineer Ayşen Aktürk who supported me throughout my lab trials with the use of Electrospinning instrument.

I am grateful for my dear friends Zeynep Selin Başaran, Övgü Gürer, Gülenay Üzüm and Ali Yılmaz for their support.

Lastly, I am also thankful to my dearest parents Sümbül Metin and Aydın Metin, as well as my dearest brother Mustafa Metin and partner Burç Erdil who morally supported me throughout this journey.

July 2020

Ayşe METİN  
(Chemist)

This study was supported by the Scientific Research Projects Coordination Unit of Istanbul Technical University. Project Number: 42361 Project Code: MYL-2019-42361



## TABLE OF CONTENTS

	<u>Page</u>
<b>FOREWORD</b> .....	<b>vii</b>
<b>TABLE OF CONTENTS</b> .....	<b>ix</b>
<b>ABBREVIATIONS</b> .....	<b>xi</b>
<b>SYMBOLS</b> .....	<b>xiii</b>
<b>LIST OF TABLES</b> .....	<b>xv</b>
<b>LIST OF FIGURES</b> .....	<b>xvii</b>
<b>SUMMARY</b> .....	<b>xxi</b>
<b>ÖZET</b> <b>xxv</b>	
<b>1. INTRODUCTION</b> .....	<b>1</b>
<b>2. THEORETICAL STUDY</b> .....	<b>3</b>
2.1 Electrospinning Process .....	3
2.1.1 Solution conductivity .....	4
2.1.2 Polymer concentration .....	4
2.1.3 Solvent volatility .....	4
2.1.4 Temperature and humidity .....	5
2.1.5 Applied voltage .....	5
2.1.6 Tip to collector distance .....	5
2.1.7 Flow rate of polymer solution .....	5
2.2 Drug Delivery Systems .....	6
2.3 Polymers Used in Nanofiber Production .....	7
2.4 Poly ( $\omega$ -pentadecalactone- <i>co</i> - $\epsilon$ -caprolactone) .....	8
2.5 Natural Polymers Used in Biomedical Applications .....	9
2.6 Gelatin .....	10
2.7 Solvents for electrospinning process .....	11
2.8 Tetracycline Hydrochloride .....	13
<b>3. MATERIALS AND METHOD</b> .....	<b>15</b>
3.1 Materials .....	15
3.2 Method .....	16
3.2.1 Enzymatic synthesis of poly( $\omega$ -pentadecalactone- <i>co</i> - $\epsilon$ -caprolactone) .....	16
3.2.2 Preparation of poly(PDL-CL)/gelatin blends .....	16
Method-1 .....	16
Method-2 .....	17
3.2.3 Electrospinning process of copolymer/gelatin blends .....	17
3.2.4 Cross-linking of the most efficient copolymer/gelatin nanofibers .....	18
3.3 Preparation of pH 7.4 phosphate buffered saline (PBS) for degradation test ..	18
3.3.1 <i>In Vitro</i> degradation tests of cross-linked copolymer/gelatin nanofibrous membranes .....	18
3.3.2 Fabrication of drug loaded copolymer/gelatin nanofibrous membranes ..	19
3.3.3 Electrospinning process of drug loaded copolymer/gelatin nanofibrous membranes .....	19
3.3.4 Cross-linking of drug loaded copolymer/gelatin nanofibrous membranes	20

3.4 <i>In vitro</i> drug release experiments of drug loaded copolymer/gelatin nanofibrous membranes .....	20
3.5 Disk diffusion method for observation of antibacterial properties of drug loaded copolymer/gelatin nanofibrous membranes .....	21
3.5.1 Preparation of mueller-hinton agar medium (MHA) .....	21
3.5.2 Disk diffusion method for investigation of antibacterial properties of membranes .....	22
3.6 Characterization Techniques .....	23
3.6.1 Scanning electron microscope(SEM) and energy-dispersive X-Ray spectrometer(EDS).....	23
3.6.2 Ultraviolet (UV) spectrophotometer .....	23
3.6.3 Fourier transform infrared spectroscopy (FTIR) .....	23
3.6.4 Differential scanning calorimetry (DSC).....	24
3.6.5 Thermal gravimetric analysis (TGA).....	24
3.6.6 Water contact angle .....	24
<b>4. RESULTS AND DISCUSSION .....</b>	<b>25</b>
4.1 Fabrication of Electrospun Copolymer/Gelatin Nanofibers .....	25
4.2 Crosslinking of The Most Efficient Copolymer/Gelatin Nanofibrous Membranes.....	27
4.3 <i>In vitro</i> Degradation Test of Cross-linked Copolymer/Gelatin Nanofibrous Membranes.....	29
4.4 Fabrication of Drug Loaded Electrospun Copolymer/Gelatin Nanofiber Membranes.....	37
4.5 <i>in vitro</i> Drug Release Studies of Copolymer/Gelatin Nanofibrous Membrane	38
4.6 Antibacterial Activity Tests for Drug Loaded Copolymer/Gelatin Nanofibers	40
4.7 FTIR Results of 0.5% Drug Loaded Copolymer/Gelatin Nanofibers.....	42
4.8 DSC Results of 0.5% Drug Loaded Copolymer/Gelatin Nanofibers.....	43
4.9 TGA Results of 0.5% Drug Loaded Copolymer/Gelatin Nanofibers .....	44
<b>5. CONCLUSIONS AND RECOMMENDATIONS .....</b>	<b>45</b>
<b>CURRICULUM VITAE .....</b>	<b>55</b>

## ABBREVIATIONS

<b>3-APTES</b>	: 3-aminopropyltriethoxysilane
<b>AA</b>	: Acetic Acid
<b><i>B. Subtilis</i></b>	: <i>Bacillus subtilis</i>
<b>CALB</b>	: Candida antarctica lipase B
<b>CFU</b>	: Colony-forming unit
<b>CL</b>	: Chloroform
<b>DMF</b>	: <i>N,N</i> -Dimethylformamide
<b>DSC</b>	: Differential scanning calorimetry
<b><i>E.Coli</i></b>	: <i>Escherichia coli</i>
<b>EDS</b>	: Energy-dispersive X-ray spectroscopy
<b>Formic Acid</b>	: Formic acid
<b>FTIR</b>	: Fourier Transform Infrared Spectroscopy
<b>HFIP</b>	: 1,1,1,3,3,3-Hexafluoro-2-propanol
<b>MHA</b>	: Mueller-hinton agar
<b>PBS</b>	: Phosphate-buffered saline
<b>PCL</b>	: Poly( $\epsilon$ -caprolactone)
<b>PEO</b>	: Poly(ethylene glycol)
<b>PEVA</b>	: Poly(ethylene vinyl acetate)
<b>PLGA</b>	: Poly(lactic-co-glycolic acid)
<b>PPDL</b>	: Poly(pentadecalactone)
<b>RHA</b>	: Rice husk ash
<b><i>S. auerus</i></b>	: <i>Staphylococcus aureus</i>
<b>SEM</b>	: Scanning Electron Microscope
<b>TFP</b>	: Tri(2-furyl)phosphine
<b>TGA</b>	: Thermogravimetric analysis
<b>UV</b>	: Ultraviolet
<b>v:v</b>	: Volume to volume ratio
<b>Wt%</b>	: Weight percent
<b>X-Ray</b>	: X-Ray diffraction



## **SYMBOLS**

<b>T<sub>m</sub></b>	: Melting temperature
<b>T<sub>g</sub></b>	: Glass-transition temperature
<b>Cl</b>	: Chlorine
<b>N</b>	: Nitrogen
<b>S</b>	: Sulfur
<b>μL</b>	: Microliter
<b>mL</b>	: Mililiter
<b>%</b>	: Percentege



## LIST OF TABLES

	<u>Page</u>
<b>Table 2.1</b> : Summary of electrospinning parameters. ....	<b>5</b>
<b>Table 2.2</b> : Most widely polymers used in electrospinning(Huang et al., 2003). ....	<b>7</b>
<b>Table 2.3</b> : Natural polymers and sources(Soares et al., 2018). ....	<b>10</b>
<b>Table 2.4</b> : Amino acids in hydrolysis collagen. ....	<b>11</b>
<b>Table 2.5</b> : Properties of some solvents used in electrospinning. ....	<b>12</b>
<b>Table 3.1</b> : Summary of blends ratio and % concentration for method-1.....	<b>16</b>
<b>Table 3.2</b> : Summary of blends ratio and % concentration for method-2.....	<b>17</b>
<b>Table 4.1</b> : Result of antibiotic release. ....	<b>39</b>



## LIST OF FIGURES

	<u>Page</u>
<b>Figure 2.1</b> : Typical electrospinning setup(Anu Bhushani and Anandharamakrishnan, 2014). .....	4
<b>Figure 2.2</b> : Polymers for electrospinning process(Bhardwaj and Kundu, 2010b) ...	7
<b>Figure 2.3</b> : Monomers structure of copolymer, from left to right: Caprolactone, Pentadecalactone. ....	8
<b>Figure 2.4</b> : Structure of gelatin.....	11
<b>Figure 2.5</b> : Molecular structure of 1,1,1,2,2,2-hexafluoro-2-propanol. ....	12
<b>Figure 2.6</b> : Molecular structure of tetracycline hydrochloride.....	13
<b>Figure 3.1</b> : Blend before electrospinning process. ....	17
<b>Figure 3.2</b> : Image of nanofibers after electrospinning. ....	18
<b>Figure 3.3</b> : Water shaking bath for degradation test of membranes.....	19
<b>Figure 3.4</b> : Electrospinning Instrument (Inovenso, Nanospinner 24). ....	20
<b>Figure 3.5</b> : Calibration graph of drug release.....	21
<b>Figure 3.6</b> : UV spectrophotometer (UV mini 1240 SHIMADZU). ....	23
<b>Figure 4.1</b> : Scanner Electron Microscope(SEM) images of 15wt.% copolymer/8wt.% gelatin (50:50) (A), 15wt.% copolymer/15wt.% gelatin (50:50) (B), 15wt.% copolymer/8wt.% gelatin (70:30) (C), 15wt.% copolymer/15wt.% gelatin (70:30) (D), 30 wt.% copolymer/8 wt.% gelatin (70:30) (E) nanofibers.....	25
<b>Figure 4.2</b> : Diameter distribution of 15wt.% copolymer/8wt.% gelatin(50:50) (A), 15wt.% copolymer/15wt.% gelatin(50:50) (B), 15wt.% copolymer/8wt.% gelatin (70:30)(C), 15 wt.% copolymer/15wt.% gelatin (70:30)(D), 30wt.% copolymer/8wt.% gelatin (70:30)(E) nanofibers.....	26
<b>Figure 4.3</b> : SEM images of 15 wt.% copolymer (A), 15 wt.% copolymer/8 wt.% gelatin (70:30) (B),15 wt.%copolymer /8 wt.% gelatin (60:40) (C), 15 wt.% copolymer /8 wt.% gelatin (50:50) nanofibers (D).....	27
<b>Figure 4.4</b> : Diameter distribution of 15 wt.%copolymer(A), 15 wt.%copolymer/8wt.% gelatin (70:30) (B),15 wt.%copolymer/8wt.% gelatin (60:40) (C), 15 wt.%copolymer/8wt.%gelatin (50:50) nanofibers (D). ....	27
<b>Figure 4.5</b> : Images of non-crosslinked-control (1), 2 hours crosslinked (2), 24 hours crosslinked (3), copolymer/gelatin nanofibrous membrane.....	28
<b>Figure 4.6</b> : SEM images of 2 hours cross-liked (A), 24 hours crosslinked(B), nanofibrous membranes. ....	29
<b>Figure 4.7</b> : Diameter distribution of 2 hours cross-liked (A), 24 hours crosslinked(B), nanofibrous membranes.....	29
<b>Figure 4.8</b> : From left to right non-crosslinked-control, 2 hours crosslinked, 24 hours crosslinked nanofibrous membranes .....	30
<b>Figure 4.9</b> : Degradation curve of 2hours crosslinked copolymer/gelatin nanofibrous membrane in PBS solution.....	31
<b>Figure 4.10</b> : 2 h cross-linked copolymer/gelatin nanofibrous membrane at the end of 30 <sup>th</sup> day of degradation test: (A) 5000x and (B) 10000x magnification.....	31

<b>Figure 4.11</b> : FTIR spectra of 2h cross-linked copolymer/gelatin nanofiber at its initial state(A) and at the end of 30 <sup>th</sup> day(B), copolymer/gelatin nanofiber(C) copolymer powder (D), 4000-600 cm <sup>-1</sup> .....	<b>32</b>
<b>Figure 4.12</b> : FTIR spectra of 2h cross-linked copolymer/gelatin nanofiber at its initial state(A) and at the end of 30 <sup>th</sup> day(B), copolymer/gelatin nanofiber(C) copolymer powder (D), 1000-1800 cm <sup>-1</sup> .....	<b>33</b>
<b>Figure 4.13</b> : Water contact angle measurements of copolymer powder (A), copolymer/gelatin nanofiber(B), 2 hours crosslinked copolymer/gelatin nanofiber(C), 24 hours crosslinked copolymer/gelatin nanofiber.....	<b>33</b>
<b>Figure 4.14</b> : Melting temperatures of samples: DSC second heating curves, crosslinked copolymer/gelatin nanofiber (A), copolymer powder (B), copolymer/gelatin nanofiber(C).....	<b>34</b>
<b>Figure 4.15</b> : DSC second heating curve of copolymer powder, Glass transition temperatures. ....	<b>34</b>
<b>Figure 4.16</b> : DSC second heating curve of copolymer/gelatin nanofiber, Glass transition temperature.....	<b>35</b>
<b>Figure 4.17</b> : DSC second heating curve of 2 h cross-linked copolymer/gelatin nanofiber: Glass transition temperature. ....	<b>35</b>
<b>Figure 4.18</b> : TGA results of copolmer powder, copolymer/gelatin nanofiber, and 2 h crosslinked copolymer/gelatin nanofiber: weight loss (A). ....	<b>36</b>
<b>Figure 4.19</b> : TGA results of copolmer powder, copolymer/gelatin nanofiber, and 2 h crosslinked copolymer/gelatin nanofiber: (B) first derivative of weight.....	<b>36</b>
<b>Figure 4.20</b> : SEM images of drug loaded copolymer/gelatin nanofibrous membranes before and after cross-linking: 0.5(A), 1(B), 3(C), 5(D) wt.% tetracycline loading ratios, copolymer/gelatin nanofiber(E), EDS analysis of 0.5 wt.% drug loaded and cross-linked nanofibrous membrane(F).....	<b>38</b>
<b>Figure 4.21</b> : Drug release graph of drug loaded copolymer/gelatin nanofibrous membrane.....	<b>39</b>
<b>Figure 4.22</b> : SEM images obtained at the end of 14-days drug release: (a) 0.5, (b) 1, (c) 3, (d) 5 wt.% tetracycline loading.....	<b>40</b>
<b>Figure 4.23</b> : Antibacterial activities of (a) 0.5, (b) 1, (c) 3, and (d) 5 wt. % antibiotic loaded samples against <i>S. aureus</i> , <i>B. subtilis</i> , and <i>E. coli</i> . (Each petri dish includes a control and three replicate disks.).....	<b>41</b>
<b>Figure 4.24</b> : Comparison of diameter of inhibition zones.....	<b>41</b>
<b>Figure 4.25</b> : FTIR spectra of cross-linked copolymer/gelatin and cross-linked TCH loaded copolymer/gelatin nanofibers (a) full spectra, (b) spectra between 1700-1500 cm <sup>-1</sup> and (c) molecular structure of TCH. ....	<b>42</b>
<b>Figure 4.26</b> : DSC results of cross-linked neat and TCH-loaded copolymer/gelatin nanofibers.....	<b>43</b>
<b>Figure 4.27</b> : TGA results of cross-linked neat and TCH-loaded copolymer/gelatin nanofibers.....	<b>44</b>





# CONTROLLED RELEASE OF TETRACYCLINE HYDROCHLORIDE FROM COPOLYMER/GELATIN NANOFIBERS

## SUMMARY

Use of nanofibers in biomedical applications have been rising significantly in recent years. Drug delivery systems are developed in order to enable the drug to perform with maximum therapeutically efficiency by preventing the degradation before the targeted spot and ensuring the protection of activation. Besides, drug delivery systems protect the body from the adverse effects of the active pharmaceutical ingredient. Conventionally, drug is given to the body by different methods such as injection, oral, implantation etc. When drug is used by these methods, it effects both the healthy and unhealthy organs. Also, conventional drug formulations cause quick release and quick removal from the body. Therefore, in most cases multiple dose is needed for healing. Multiple dose increases the toxic effects and may result in the occurrence of side effects.

Recently, the importance of developing drug delivery systems with controlled release and controlled targeted spot release have risen significantly. Studies prove the success of polymeric drug delivery systems in controlled release. Electrospinning is the most frequently used method to obtain nanofiber. In this method, natural or synthetic polymer solutions are spinned under electric force in order to achieve nanofibers from 2nm up to a few micro-meters. Nanofibers presents great advantages for drug delivery systems due to their special properties such as high surface-volume ratio, pore structure, high permeability, easy penetrability and biocompatibility achieved by using natural polymers.

Aliphatic polyesters synthesized with enzymatic ring opening polymerization do not generate a toxicity risk because of the method of synthesis without a catalyst and can be used in drug delivery systems. Enzymatically synthesized poly( $\omega$ -pentadecalactone-co- $\epsilon$ -caprolactone) has been chosen as the polymer in this study because of its biocompatibility, biodegradability and good mechanical strength properties. Due to the improvement of mechanical and degradation properties and hydrophobic structure, prevention of uncontrolled water release was expected from nanofibers synthesized from poly ( $\omega$ -pentadecalactone-co- $\epsilon$ -caprolactone) copolymers by immobilizing lipase enzyme on rice husk ashes as the method found in literature. Besides, gelatin which is a natural polymer was used in order to achieve easier acceptance of drug release system by the body and increase the compatibility with human cell.

Nanofiber membranes obtained with a lab scale electrospinning machine from various copolymer/gelatin concentrations and volume-wise several double mixture compositions were studied in two different solvent systems as the first step of the study. Chloroform and methanol (3:1 v, v) for copolymer, acetic acid and formic acid (1:1 v, v) for gelatin were chosen as the first solvent system. 15% and 30% by weight for copolymer and 8% and 15% by weight for gelatin were prepared in solution. Afterwards, obtained solutions were mixed with various volume ratios. The achieved mixtures were electrospinned using syringe for transfer. Phase separation was observed when the mixture was leaving the syringe during electrospinning process. Nanofibers obtained from the first solvent system were viewed by scanning electron microscope (SEM). Beaded and defected structure was observed on the membrane

because of the phase separation. Increasing copolymer concentration in double mixtures resulted in increased beaded structure with a few nanofibers in between. Besides, an increase from 8% to 15% in weight of gelatin concentration increased the defects as well.

A new solvent system has been researched in order to prevent the defects in the structure. As a result of this research, hexafluoroisopropanol; a solvent which can dissolve both the copolymer and gelatin, was chosen for the second solvent system. 15% copolymer and 8% gelatin solutions by weight were prepared and mixed with various volume ratios (100:0, 70:30, 60:40, 50:50). As a result of SEM images, electrospinning of 50:50 volume ratio mixture of 15% copolymer and 8% gelatin solutions had the best fiber structure and the best fiber diameter distribution (average fiber diameter:  $305.0 \pm 45.5$  nm). Membranes obtained with this ratio were used on the next steps of the study because of it having the most effective and the most proper structure. In order to increase the mechanical properties and the stability of the membranes, they were crosslinked for 2 and 24 hours in glutaraldehyde vapour. Then, *in vitro* degradation properties were examined in pH 7.4 phosphate buffer solution. 2 hours crosslinked membrane preserved its structure in phosphate buffer solution after 30 days. Degradation tests proved that 2 hours crosslinked membrane had high hydrolytic resistance against buffer solution. Even though 24 hours crosslinked membrane had better mechanical resistance, 2 hours crosslinked membranes were chosen because of the higher toxicity of 24 hour crosslinked membrane due to higher glutaraldehyde ratio. 2 hours crosslinked membrane was placed to shaking bath in buffer solution and mass loss was calculated in various time intervals (1, 3, 5, 7, 14, 21, 30 days). Membrane has lost the 20% of its initial mass after 10 days. Copolymer/gelatin nanofiber, 2 hours crosslinked copolymer/gelatin nanofiber and copolymer have been analysed by fourier transform infrared spectroscopy (FTIR), thermal gravimetric analysis (TGA), differential scanning calorimetry (DSC) and contact angle measurement. As a result of contact angle measurement 2 hours crosslinked membrane was found suitable because it preserved its hydrophilic properties and improved its hydrolytic properties compared to non-crosslinked membrane. An increase in thermal resistance properties of the membrane was observed according to TGA results. As the second step of the study, calculated amount of Tetracycline Hydrochloride antibiotic was dissolved in HFIP. The amount of drug was arranged as 0.5%, 1%, 3% and 5% of the total polymer/gelatin concentration by weight. Drug loaded nanofiber membranes were obtained by electrospinning the mixture with 2ml/hour flow rate and under 25kV room temperature conditions. Afterwards, membrane was crosslinked for 2 hours in 25% glutaraldehyde solution vapour. Crosslinked nanofibers were dried for 2 hours in 80°C in order to remove remaining glutaraldehyde. After the crosslinking process, drug loaded copolymer/gelatin nanofiber membranes were cut in to  $2 \times 2$  cm<sup>2</sup> pieces and weighed. 3 samples were prepared as described for each drug loading ratio and these samples were sunk in 10 ml pH 7.4 phosphate buffer saline (PBS). Later on, samples were placed in 37°C shaking bath(120rpm). 1ml parts were taken of and changed with fresh PBS in determined time intervals. Removed mixtures were characterized by using UV spectrophotometer in 343nm. Amount of drug released was calculated by using calibration graph. Later on, cumulative drug release amount was reached. Initial drug amount in the membrane was calculated according to the drug ratio in polymer blend and the weight of the drug loaded membrane. SEM images of drug loaded nanofibers proved that, randomly aligned, even and beadless antibiotic loaded samples for each ratio were obtained. Fiber diameters showed normal distribution generally. A tendency

in the decrease of diameter was observed after drug loading. Highest average nanofiber diameter ( $282.9 \pm 64.6$  nm) was measured in the lowest drug loading ratio (0.5% by weight). Other drug loading ratios (1%, 3% and 5% by weight) caused the formation of significantly thinner nanofibers (180-200 nm) ( $p < 0.001$ ). On the other hand, there was no meaningful diameter difference between 3 drug loaded samples ( $p > 0.05$ ). EDS spectrum of 0.5% by weight drug loaded and crosslinked membrane was obtained in order to determine the presence of tetracycline hydrochloride in drug loaded copolymer/gelatin nanofiber structure. Cl spectrum has verified the presence of tetracycline hydrochloride because Chloride (Cl) is made up of the molecular structure of tetracycline hydrochloride. Additionally, nitrogen (N) and sulphur (S) peaks were detected in EDS spectrum. These peaks proved the presence of gelatin in nanofibers. Cumulative drug release graph showed that, instant release and 14th day release for each drug load were similar to each other. For each drug load ratio, instant release in 1 hour was less than 11%. On the other hand, 0.5% by weight drug loaded sample displayed relatively low instant release percentage ( $\% 9.1 \pm 0.1$ ) and highest ( $p < 0.001$  or  $p < 0.05$ ) total drug release percentage ( $\% 69.4 \pm 0.2$ ). 0.5% ratio drug having low instant release and highest gradual total drug release was determined as the most efficient antibiotic ratio for copolymer/gelatin ratio developed at this stage of the study.

As the next stage of the study, antibacterial tests of the antibiotic loaded nanofibers were performed by using disk diffusion method; which is the measurement of the bacterial growth inhibition zones for the determination of antibacterial activity. Antibacterial activities were tested against Gram positive (*S. aureus* and *B. subtilis*) and Gram negative (*E. coli*) bacteria. Results showed that all samples with various loading ratios presented open inhibition zones against Gram positive bacteria (*S. aureus* and *B. subtilis*). Bigger inhibition zones were monitored in petri dishes with *B. subtilis* ( $\sim 30$ - $40$  mm). This result proved that drug loaded membranes were extremely active and effective against *B. subtilis*. Meanwhile, samples showed limited activity against *E. coli*. No inhibition zone was detected for 0.5% by weight tetracycline hydrochloride and samples with higher concentrations showed very low antibacterial activity ( $\sim 8$ - $10$  mm inhibition zone). It was found that; parallel with the literature, Gram negative bacteria *E. coli* was much more resistant to tetracycline hydrochloride antibiotic. Additionally; as expected, inhibition zones expanded as the antibiotic concentration increased. Optimal antibiotic ratio; obtained by release properties, was determined as 0.5%. 0.5% antibiotic ratio had enough efficacy for gram positive bacteria, however for broad spectrum antibiotic, antibiotic loading ratio has to be increased.

In this study, increase of the mechanical properties by using enzymatically synthesized copolymer and increase of cell compatibility by using a natural polymer gelatin while obtaining nanofiber with electrospinning process were targeted. Nanofiber membrane with the optimal structure was successfully achieved by trying various copolymer/gelatin ratios and different solvents. Crosslinked samples were characterized without drug loading in order to increase the mechanical properties and degradation properties were examined. At the final step of the study, controlled release properties of antibiotic loaded membranes with various ratios has been examined and their activity against bacteria was measured.



## KOPOLİMER/JELATİN NANOLİFLERİNDEN TETRASİKLİN HİDROKLORÜRÜN KONTROLLÜ SALINIMI

### ÖZET

Son yıllarda biyomedikal uygulamalarda nanoliflerin kullanılmasına olan ilgi gün geçtikçe artmaktadır. İlaç taşınım sistemleri, ilaçların maksimum iyileştirme özelliği gösterebilmesi için hedeflenen bölgeden önce bozunmasını engellemek ve aktivasyonunun korumasını sağlamak için geliştirilmektedir. Ayrıca ilaç taşıma sistemleri vücudu ilaç etken maddesinin olumsuz etkilerinden korur. İlaç taşıma sistemleri, ilacın etkinliğini arttıran polimer veya lipid taşıyıcı sistemlerdir. Bu sistemlerde, ilacın salım süresini ve hızını geliştirerek, ilacın hedef bölgeye ulaşması sağlanır. Geleneksel olarak ilaç vücuda enjeksiyon, oral sindirim, implantasyon gibi yöntemlerle verilir. İlaç bu yöntemlerle vücuda alındığında hem sağlıklı hem de sağlıklı organ ve hücreleri etkiler. Ayrıca geleneksel ilaç formülasyonları hızlı salıma neden olur ve ilaç vücuttan hızlı bir şekilde atılır. Bu nedenle iyileşme için çoğu zaman çoklu dozlama gerekir. Bu da toksik etkileri artırır ve ilacın yan etkilerinin ortaya çıkmasına neden olabilir.

Son yıllarda kontrollü salım sağlayan ve hedeflenen bölgede ilacın salımını kontrol edebilen ilaç taşıma sistemleri geliştirmek oldukça önem kazanmıştır. Yapılan çalışmalar, polimerik ilaç taşınım sistemlerinin kontrollü salımda başarısını göstermektedir. İlaç etken maddenin polimer matrisine hapsedilebilmesi için birçok yöntem bulunmaktadır. Bu yöntemlerden bazıları polimerden film eldesi, emülsiyon tekniği, sprey kurutma yöntemi, polimer jeller ve elektro-eğirme yöntemidir. Elektro-eğirme yöntemi nanolif elde etmek için en sık kullanılan yöntemlerden biridir. Bu yöntemde 2nm ile birkaç mikrometre arasında çaplara sahip nanolifler elde etmek için, elektrik kuvveti altında doğal ve/veya sentetik polimer çözeltileri eğrilir. Nanolifler ilaç taşınım sistemleri için, yüksek yüzey-hacim oranı, gözenekli yapı, yüksek geçirgenlik, kolay işlenebilirlik ve doğal polimer çözeltileri de kullanarak elde edilebilen biyouyumluluk gibi özellikler sayesinde üstün avantajlar sunar. Ayrıca nanolif yapısı vücutta bölgeye özgü taşınımı mümkün kılan ekstraselüler matriksi taklit eder. Nanolif yapıdaki taşınım sistemlerinin bir diğer avantajı ise birden fazla ilaç aynı lifli taşıyıcıya kapsüllenebilir. İlaç taşınım sistemlerinde yaygın olarak poli (vinil alkol), poli (etilen oksit), poli ( $\epsilon$ -kaprolakton), kitosan, jelatin gibi doğal ve sentetik polimerler kullanılabilir. İlaç salım mekanizması polimer özelliklerine ve ilaç-polimer etkileşimine göre değişir.

Enzimatik halka açılma polimerizasyonu ile sentezlenen alifatik poliesterler kimyasal katalizör kullanılmadan sentezlendiğinden, toksisite riski oluşturmaz ve ilaç taşınım sistemlerinde kullanılabilir. Bu çalışmada biyouyumluluk, biyobozunurluk, iyi mekanik dayanım özelliklerinden dolayı, enzimatik olarak sentezlenmiş poli ( $\omega$ -pentadecalakton-ko- $\epsilon$ -kaprolakton) seçildi. Daha önce literatürde bulunan yöntemle başarı ile pirinç kabuğu külleri üzerine immobilize edilmiş lipaz enzimi yoluyla sentezlenen poli ( $\omega$ -pentadecalakton-ko- $\epsilon$ -kaprolakton) kopolimerinden, nanoliflerin mekanik ve bozunma özelliklerini geliştirmesi ve hidrofobik yapısının sonucu olarak kontrolsüz su salınımını engellemesi beklendi. Ayrıca ilaç salım sisteminin vücut tarafından kolayca kabul edilmesine yardımcı olması, hücre ile uyumluluğunu arttırması ve ilacın bölgeye özgü taşınmasını geliştirmesi için doğal bir polimer olan

jelatin kullanıldı.

Çalışmanın ilk aşamasında, 2 farklı çözücü sisteminde çeşitli kopolimer/jelatin konsantrasyonları ve hacimce çeşitli ikili karışım kompozisyonları çalışılarak, laboratuvar ölçekli bir elektro-eğirme cihazı ile nanolif membranlar elde edildi. İlk çözücü sistemi olarak kopolimer için Kloroform ve Metanol (3:1 v, v), jelatin için Asetik Asit ve Formik Asit (1:1 v, v) çözücüleri seçilmiştir. Kopolimer için ağırlıkça %15, %30, jelatin için ağırlıkça %8, %15 çözeltileri hazırlandı. Daha sonra elde edilen çözeltiler çeşitli hacim oranlarında karıştırıldı. Elde edilen karışımlar şırıngaya aktarılarak elektro-eğirme işlemine tabi tutuldu. Elektro-eğirme işlemi sırasında şırıngada çözeltilerin faz ayırmasına uğradığı gözlemlendi. İlk çözücü sisteminden elde edilen nanolifler taramalı elektron mikroskopisi (SEM) ile görüntülendi. Faz ayrımı nedeniyle membranda boncuklu ve kusurlu yapı gözlemlendi. İkili karışımlarda artan kopolimer konsantrasyonu, aralarında birkaç nanolif bulunan çok daha fazla boncuk oluşumu ile sonuçlandı. Ayrıca, jelatin konsantrasyonunda ağırlıkça %8'den %15'e kadar artış kusurları arttırdı.

Yapıdaki hataların önüne geçmek için ikinci bir çözücü sistemi araştırıldı. İkinci çözücü sistemi için hem kopolimeri hem de jelatini çözebilen Heksafluoroizopropanol çözücüsü seçildi. Ağırlıkça %15'lik kopolimer ve %8'lik jelatin çözeltileri hazırlanarak hacimce çeşitli oranlarda (100:0, 70:30, 60:40, 50:50) karıştırıldı. SEM görüntülerinden elde edilen bilgiye göre, en düzgün lif yapısına ve en iyi lif çapı dağılımına %15 kopolimer, %8 jelatin çözeltilerinin hacimce 50:50 karıştırılması ve elektro-eğirmesi ile ulaşıldı (ortalama lif çapı:  $305.0 \pm 45.5$  nm). Çalışmanın diğer basamaklarına en düzgün ve etkili yapıya sahip, bu orandaki karışımdan elde edilen membranlar ile devam edildi. Membranların mekanik özelliklerini geliştirmek ve kararlılığını arttırmak için Gluteraldehit buharında 2 ve 24 saatlik çapraz bağlama çalışmaları yapıldı. Daha sonra pH 7,4 fosfat tampon çözeltisi içinde, in vitro bozunma özellikleri incelendi. 2 saat çapraz bağlanmış membran Fosfat tampon çözelti içinde 30 günün sonunda yapısını korudu. Degradasyon testleri, 2 saatlik çapraz bağlı membranın tampon çözeltiye karşı yüksek hidrolitik dirence sahip olduğunu gösterdi. 24 saatlik çapraz bağlama prosesi daha iyi mekanik dayanım gösterse de, yüksek gluteraldehit oranı membranların toksitesinin artmasına neden olacağından 2 saatlik çapraz bağlama yeterli görüldü ve çalışmalara bu membran ile devam edildi. 2 saat çapraz bağlı membran tampon çözelti içinde çalkalama suyu banyosuna yerleştirildi ve kütle kaybı belirli zaman aralıklarında (1, 3, 5, 7, 14, 21, 30. gün) hesaplandı. Membran 10 gün sonunda başlangıç kütesinin %20'sini kaybetti. Kopolimer/jelatin nanolif, 2 saat çapraz bağlanmış kopolimer/jelatin nanolif ve kopolimer, fourier dönüşümlü kızılötesi spektroskopisi (FTIR), termal gravimetrik analiz (TGA), diferansiyel taramalı kalorimetri (DSC) ve temas açısı ölçümü ile karakterize edildi. Temas açısı ölçümü sonucu 2 saat çapraz bağlanmış membranın ilaç salım için uygun olan hidrofilik özelliğini koruduğunu, aynı zamanda çapraz bağlı olmayan membrana göre hidrolitik direncinin geliştiğini göstermektedir. DSC sonuçlarına göre karışımda jelatinin bulunması Erime Sıcaklığını ( $T_m$ ) ve Camsı Geçiş Sıcaklığını ( $T_g$ ) düşürdüğünü, membranın çapraz bağlanmasının ise  $T_m$  ve  $T_g$ 'yi arttırdığını göstermektedir. TGA sonuçlarına göre çapraz bağlanma sonucunda, membranın termal dayanım özelliklerinin geliştiği gözlemlendi.

Çalışmanın ikinci aşamasında hesaplanan miktarda Tetrasiklin Hidroklorür antibiyotiği, HFIP içerisinde çözüldürüldü. İlaç miktarı, toplam polimer/jelatin konsantrasyonunun ağırlıkça % 0.5, 1, 3 ve %5'i olacak şekilde düzenlendi. Çözelti 2ml/saat akış hızında, 25 kV altında çevre koşullarında elektro-eğirme işlemine tabi

tutularak ilaç yüklenmiş nanolif membranlar elde edildi. Çapraz bağlama prosesinden önce membran yapısında kalmış olabilecek çözücüyu uzaklaştırmak için membran 24 saat boyunca 30°C'de kurutuldu (0.1 mm kalınlık). Daha sonra membran 2 saat %25'lik glutaraldehit çözeltisi buharında çapraz bağlandı. Çapraz bağlı nanolifler, artık Glutaraldehit'den kurtulmak için 80 °C'de 2 saat kurutuldu. Çapraz bağlamadan sonra, ilaç yüklü kopolimer / jelatin naolif membranlar 2 x 2 cm<sup>2</sup> boyutunda kesildi ve tartıldı. Her ilaç yükleme oranı için, tarif edildiği gibi 3 numune hazırlanıp ve 10 ml pH 7.4 fosfat tamponlu Salin (PBS) içine batırıldı. Daha sonra, numuneler 37°C'de çalkalamalı su banyosuna (120rpm) konuldu. Belirlenen zaman periyotlarında, 1 ml'lik kısımlar çıkarıldı ve taze PBS ile değiştirildi. Çıkarılan çözeltiler, 343 nm'de UV spektrofotometre kullanılarak karakterize edildi. Serbest bırakılan ilacın miktarı kalibrasyon grafiği kullanılarak hesaplandı. Daha sonra, kümülatif ilaç salım miktarına ulaşıldı. Membranda mevcut olan ilk ilaç miktarı, polimer harmanındaki ilaç yüzdesine ve ilaç yüklü membranın ağırlığına göre hesaplandı. İlaç yüklü nanoliflerin SEM görüntüleri gösterdi ki, Her oranda antibiyotik yüklü örneklerde rastgele hizalanmış, pürüzsüz ve boncuksuz nanolifler elde edildi. Lif çapları genel olarak normal dağılım gösterdi. İlaç yüklendikten sonra çapta azalma eğilimi gözlemlendi. En düşük ilaç yükleme oranında (ağırlıkça %0,5), en yüksek ortalama nanofiber çapı (282.9 ± 64.6 nm) ölçüldü. Diğer ilaç yükleme oranları (ağırlıkça %1, 3 ve %5), önemli ölçüde daha ince nanoliflerin (180-200 nm) oluşmasına yol açtı (p <0.001). Diğer yandan, ilaç yüklü bu 3 örnek arasında anlamlı bir çap farkı yoktu (p > 0.05). İlaç yüklü kopolimer/jelatin nanoliflerin yapısında tetrasiklin hidroklorürün varlığını saptamak için ağırlıkça %0.5 ilaç yüklü ve çapraz bağlı membranın EDS spektrumu elde edildi. Klorür (Cl) tetrasiklin hidroklorürün moleküler yapısından oluştuğu için, Cl spektrumu, tetrasiklin hidroklorür varlığını teyit etti. Ek olarak, EDS spektrumunda Azot (N) ve Kükürt (S) pikleri de tespit edildi ve bu da nanoliflerde jelatin varlığını kanıtladı. Kümülatif ilaç salım grafiği gösterdi ki, her orandaki ilaç yüklemesi için ani salım ve ardından 14. güne kadar kademeli salım birbirine benzerdi. 1 saat içindeki ani salım, tüm ilaç oranları için %11'den azdı. Diğer yandan, ağırlıkça %0,5 ilaç yüklü örnek, nispeten düşük ani salım yüzdesi (% 9.1 ± 0.1) ile en yüksek (p <0.001 veya p <0.05) toplam ilaç salım yüzdesini (% 69.4 ± 0.2) sergiledi. Çalışmanın bu aşamasında geliştirilen kopolimer/jelatin membran için en verimli antibiyotik oranı olarak, düşük ani salım ve kademeli olarak en yüksek toplam ilaç salımına sahip olan %0,5 oranındaki ilaç olduğu saptandı. Çalışmanın bir sonraki aşamasında, antibiyotik yüklü nanoliflerin antibakteriyel aktivite testleri, bakteriyel büyüme inhibisyon bölgesinin ölçülmesiyle antibakteriyel aktivitenin belirlendiği, disk difüzyon yöntemi kullanılarak yapıldı. Antibakteriyel aktiviteler Gram pozitif (*S. aureus* ve *B. subtilis*) ve Gram negatif (*E. coli*) bakterilere karşı test edildi. Sonuçlar, değişik antibiyotik yükleme oranlarına sahip tüm numunelerin Gram pozitif bakteri *S. aureus* ve *B. subtilis*'e karşı açık inhibisyon bölgeleri sergilediğini gösterdi. *B. subtilis* petri kaplarında daha büyük inhibisyon bölgeleri (~ 30-40 mm) gözlemlendi. Bu sonuç, ilaç yüklü membranların bu bakteriye karşı son derece aktif olduğunu gösterdi. Öte yandan, numuneler *E. coli*'ye karşı sınırlı aktivite gösterdi. Ağırlıkça %0,5 tetrasiklin hidroklorür oranı için, inhibisyon bölgesi tespit edilmedi ve daha yüksek konsantrasyonlu numuneler düşük antibakteriyel aktivite gösterdi (~ 8-10 mm inhibisyon bölgesi). Literatürle uyumlu olarak, Gram negatif bakteri *E. coli*'nin tetrasiklin hidroklorür antibiyotiğine daha dirençli olduğu bulundu. Ek olarak, inhibisyon bölgeleri beklendiği gibi artan antibiyotik konsantrasyonu ile genişledi. Salım özellikleri ile elde edilen optimum antibiyotik oranı %0,5 olarak bulundu. %0,5 antibiyotik oranı, Gram pozitif bakteriler için yeterli etkinliğe sahiptir. Fakat geniş

spektrumlu antibiyotik olarak kullanılmak istendiğinde, yüklü olan antibiyotik oranını arttırmak gerektiği sonucuna ulaşıldı.

Bu çalışmada elektro-eğirme yöntemi ile nanolif eldesinde, doğal bir polimer olan jelatin kullanılarak, hücre uyumluluğunu arttırmak, enzimatik sentezlenmiş kopolimer kullanarak da mekanik özelliklerin artırılması hedeflendi. Çeşitli kopolimer/jelatin oranları ve farklı çözücüler denenerek, optimum yapıdaki nanolif membran başarı ile elde edildi. Mekanik özellikleri daha da iyileştirmek için çapraz bağlanan numuneler ilaçsız olarak karakterize edildi ve bozunma özellikleri incelendi. Çalışmanın son basamağında, çeşitli oranlarda antibiyotik yüklenen membranların kontrollü salım özellikleri incelendi ve bakterilere karşı aktiviteleri ölçüldü. Öte yandan daha ileri bir çalışma olarak elde edilen membranlara sitotoksitite testleri çalışılabilir.







## 1. INTRODUCTION

Drug delivery systems enable the encapsulated therapeutic agents to be released into the body by increasing their effectiveness. These systems are responsible for the control a site, time and rate of drug release. Drugs more than optimal concentration cause toxicity for all living creatures. The interest on controlled drug delivery systems; one of the important research areas, has increased recently. Improved therapeutic efficacy and low toxicity are some good advantages of controlled drug delivery systems. Materials used in controlled drug delivery systems may be polymer and lipid based carrier systems. The conventional drug delivery routes include injection, oral ingestion, implantation, and transdermal delivery(Jayaraman et al, 2015). Electrospinning method is suitable for processing of natural and biocompatible synthetic polymers to achieve nanofiber(Zong et al, 2002). Electro-spun nanofibers can be used as drug carrying material. Electro-spun nanofibers provide some excellent benefit to materials such as high surface area and porous structure. Drug can be directly encapsulated to nanofiber matrix by electrospinning process(Kenawy et al, 2008.). Nanofibers exhibit surface functionalization and it can be easily fabricated from synthetic and natural polymers or their blends(Supaphol et al, 2011). Therapeutic agents such as anticancer and anti-inflammatory drugs, antibiotics, and genes can be encapsulated to nanofiber and carried to target(Supaphol et al, 2011). On the other hand, researchers have focused on to increase biocompatibility and biodegradability of nanofiber matrix. Improvement in biocompatibility may be arranged by using natural polymer and biodegradable synthetic polymer. In this study, gelatin was used as natural polymer to enhance biocompatibility of nanofiber structure. However, gelatin nanofiber is highly hydrophilic and it has poor mechanical strength. To overcome these issues, enzymatically synthesized poly ( $\omega$ -pentadecalactone-co- $\epsilon$ -caprolactone) was used as biopolymer in blend. Different copolymer/gelatin concentrations and various volume ratios blend compositions were studied in two different solvent systems and blends were spun by electrospinning. Crosslinking process was applied to optimize mechanical strength of nanofiber membranes.

Degradation behaviour of nanofiber structure was studied. Images of nanofiber membranes were obtained by SEM in nanoscale. Copolymer/gelatin, copolymer powder and crosslinked copolymer/gelatin were characterized for the comparison of differences in structure and properties by FTIR, DSC, TGA and water contact angle analysis.

In the other part of this study, different amounts of tetracycline hydrochloride antibiotic were added to the most efficient copolymer/gelatin blend. Blends were spun and crosslinked. Drug release behaviours of membranes were investigated to achieve the most efficient drug concentration in nanofiber membrane. Drug loaded membranes were scanned by SEM in order to obtain nanofiber structure. EDS mapping analysis was applied to membranes to prove that there is antibiotic in nanofiber structure. Antibacterial activities were tested against Gram positive (*S. aureus* and *B. subtilis*) and Gram negative (*E. coli*) bacteria by using disk diffusion method.

## 2. THEORETICAL STUDY

### 2.1 Electrospinning Process

Electrospinning process is mostly preferred for fiber production method which applies electrical forces to form nanofibers with diameters between 2 nm to several micrometers. The production of nanofiber from natural and synthetic polymer solutions by electrospinning method has provided a great improvement in research and economic consideration within the last ten year (Bhardwaj and Kundu 2010a). Non-woven nanofibers with excellent properties such as stability, high surface area to volume ratio, easy functionalization, high permeability, porosity and perfect mechanical properties can be achieved by electrospinning (Al-Enizi et al, 2018). Excellent properties and easy workability, makes electro-spun nanofibers exciting candidates for wide range applications such as drug delivery, tissue engineering, wound dressing, reinforcing of materials, air and dust filters, and high-performance materials (Ingavle and Leach, 2014). Typically, a setup of electrospinning instrument consists of four major parts, these are grounded collector, syringe pump, capillary tube and high voltage source (Figure 2.1). The basic principle of electrospinning is creation of a strong electrical field (Hu et al, 2014). The polymer solution is pumped through the capillary tube, then a high voltage is applied, a pendant drop of polymer solution becomes highly electrified and the induced charges are distributed over the surface (Hu et al, 2014). The liquid drop turns into "Taylor Cone". When the electric force overcomes the surface tension of the polymer solution droplet, charged solution is ejected from the tip of the Taylor cone. Solvent evaporates and nanofibers gets collected in the collector (Zeng et al, 2003). Fiber formation and structure can easily be affected by environmental, solution and process variables (Sill and von Recum, 2008). Solution parameters are solution conductivity, polymer concentration and solvent volatility. Environmental variables include temperature and humidity. Processing parameters are applied voltage, tip to collector distance and polymer flow rate (Table 2.1).

Generally, the structure of obtained electro-spun nanofibers are different than the expected one because of the effect of numerous parameter combinations and some unknown variables (Pelipenko et al, 2015).

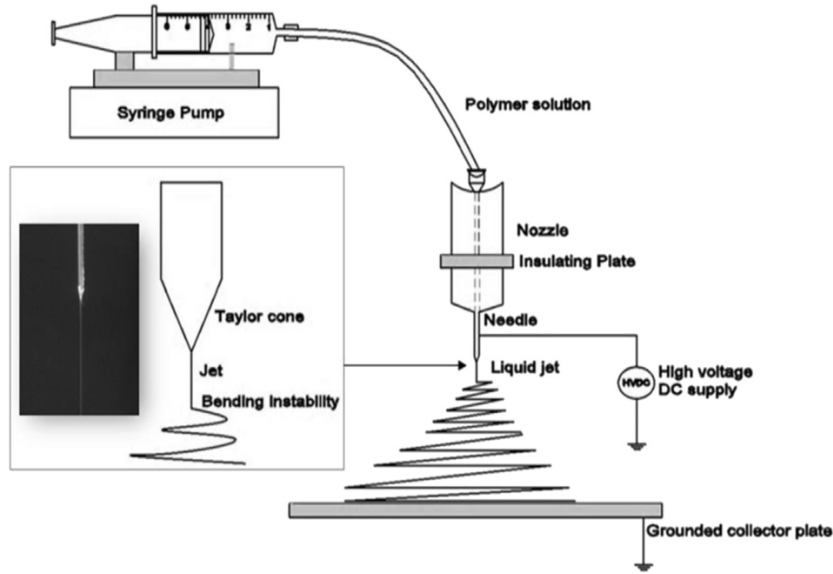


**Figure 2.1 :** Typical electrospinning setup(Anu Bhushani and Anandharamakrishnan, 2014).

### 2.1.1 Solution conductivity

Electrical charge can be carried more easily by highly conductive solutions. Using highly conductive solution is an important advantage in electrospinning process (Sill and von Recum, 2008). Bead formation in nanofiber structure can be reduced by raising solution conductivity. Additionally, increasing conductivity helps in obtaining thinner fiber formation and improves property of the fiber structure (Zong et al, 2002).

### 2.1.2 Polymer concentration

The optimum concentration value is needed for spinning the solution. Polymer concentration has effect on other electrospinning solution parameters such as viscosity. High polymer concentration causes high solution viscosity which disables the control of flow rate. On the other hand, low polymer concentration causes bead formation due to surface tension effect. Experimental researches show that increase in solution concentration increases the diameter of fiber in acceptable concentration range(Zong et al, 2002).

### 2.1.3 Solvent volatility

Fiber porosity and structure are affected by solvent volatility. Solvent must evaporate until the nanofiber reaches to the collector during electrospinning process. High volatility may cause phase separation in syringe. Flat fibers and fibers with surface pores may occur when solvent is highly volatile (Casper et al, 2004).

**Table 2.1** : Summary of electrospinning parameters.

Process	Solution	Environmental
Applied voltage	Solution conductivity	Temperature
Tip to collector distance	Polymer concentration	Humidity
Polymer flow rate	Solvent volatility	

#### **2.1.4 Temperature and humidity**

As known, when temperature increases, viscosity decreases. Some studies show that, fiber diameter may decrease with reducing viscosity(Rošić et al, 2011). Percentage of ambience humidity must be controlled during electrospinning process. In general, high value humidity (more than 30%) may cause some defaults on the surface of nanofiber. High ambience humidity increases the number of pores in surfaces. High moisture condition of the air causes big pores in a surface and it changes the morphology of nanofiber(Casper et al, 2004).

#### **2.1.5 Applied voltage**

Applied voltage is a critical parameter for electrospinning process. Fiber formation occurs after reaching critical voltage value. Different approaches have been proposed about the effect of voltage. Some studies have shown that, thick nanofibers occur when high voltage is applied (Zhang et al, 2005). However, most studies show that increasing applied voltage creates nanofibers with finer diameters. Moreover, beads and defects may be formed when high voltage is applied(Haghi and Akbari, 2007)(Katti et al, 2004).

#### **2.1.6 Tip to collector distance**

Tip to collector distance is a respectable parameter for morphology of nanofibers. Optimum distance between tip and collector is needed to enable the formation of a nanofiber with good structure. Distance should be enough to evaporate a solvent before nanofiber reaches the collector, otherwise bead formation occurs in the surface of nanofiber(Bhardwaj and Kundu, 2010a).

#### **2.1.7 Flow rate of polymer solution**

During electrospinning process, flow rate of solution must be enough to create Taylor cone. Flow rate permanency should be ensured to form stable Taylor cone. Increasing flow rate increases the diameter of fiber since there is more than required polymer solution in the needle tip (Leung and Ko, 2011).

## **2.2 Drug Delivery Systems**

Drug release velocity, area and duration of therapeutic goods in capsules are controlled by drug delivery systems, which results in increase of the efficacy (Mahato, 2007). Tissue regeneration requires the controlled release of the drug in the necessary time interval without degrading the rest of the encapsulated drug (Mahato, 2007). Optimum efficiency is achieved only by having the therapeutic agent in its best possible concentration range (Jayaraman et al, 2015). If the therapeutic good is below the desired concentration range, there will be restricted gain and if it is above there will be toxic effects to human body. Injection, oral ingestion, implantation and transdermal delivery are the conventional drug usage ways (Mahato, 2007).

Drug delivery systems are aimed to carry the therapeutic agents to the desired spot in the body in order to achieve maximum efficacy and activation without degradation when it reaches the target. Drug delivery systems are made up of either polymers or lipids and control the release velocity, area and duration of therapeutic goods in capsules. With the help of the investments, scientists focus to develop new and more efficient drug delivery methods with less or no adverse effects.

When a drug is taken in the body by the conventional methods such as injection, oral, implantation or transdermal delivery, not only the unhealthy cells get effected but therapeutic agents also effect the healthy cells and organs. In conventional methods, therapeutic agent is usually released and removed from body instantly. Therefore, multiple dosing is necessary for fully therapeutic result almost all the time (Domb and Khan, 2014a). Multiple dosing increases the risk of toxic and harmful effects, prevents a stable active ingredient level in plasma and makes it harder for the patient to comply. There have been newly patented technologies of delivery systems developed aiming for the optimum concentration range and controlled release in the past years (Domb and Khan, 2014b). These new drug delivery technologies require and therefore increase the interest on polymer based materials in order to allow the control of release velocity, duration and area. There are many different polymer forms parallel with the

end use requirements for obtaining controlled drug delivery such as hydrogel, micro/nanoparticle, nanofiber etc. There are a few requirements that needs to be studied in order to choose a material to be used as drug delivery device. One of these requirements is that the material should prevent the decomposition in blood. Necessity of biodegradation to get rid of explantation is another important requirement. Third requirement is to have a stable controlled release property at the desired speed, duration and area for the active ingredient to complete the treatment(Domb and Khan, 2014b). System also has to assure the release of the therapeutic agent only to the desired area.

### 2.3 Polymers Used in Nanofiber Production

Nanofibers can be produced by few different methods such as self-assembly, electrospinning, phase separation production methods. Most widely used materials for production of nanofibers are synthetic and natural polymers or their combinations (Figure 2.2). Combination of materials in solution or melt forms can be used in electrospinning process directly. Electrospinning process can be applied to many polymers such as polyethylene terephthalate, PBI, polystyrene, PCL, PEO, poly(2-hydroxyethyl methacrylate) and also even DNA can be spun by electrospinning process(Frenot and Chronakis, 2003) (Table 2.2).

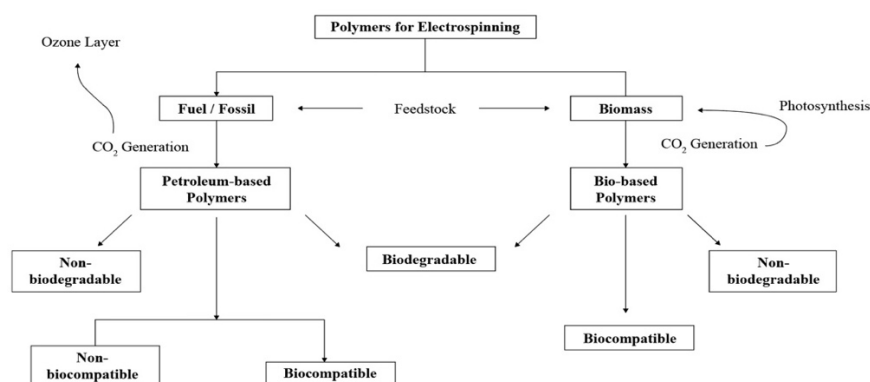


**Figure 2.2 :** Polymers for electrospinning process(Bhardwaj and Kundu, 2010b)

**Table 2.2 :** Most widely polymers used in electrospinning(Huang et al, 2003).

Polymers	Perspective applications
Nylon 6,6, PA-6,6	Protective clothing

Polyurethanes	Protective clothing and filters
Poly(acrylonitrile)	Carbon nanofiber
PEVA/PLA	Drug delivery system
Collagen-PEO	Wood dressing, tissue engineering
Polyamide	Glass fiber filter media
Poly( $\epsilon$ -caprolactone)	Drug delivery system
Poly(vinyl phenol)	Antibacterial agent

## 2.4 Poly( $\omega$ -pentadecalactone-co- $\epsilon$ -caprolactone)

As many studies have shown, synthesis of aliphatic polyesters using metal based catalysts cause toxicity. Because of toxicity they are not suitable for use in biomedical applications. Enzymes can be decent alternatives for metal based catalysts which are widely used in ring opening polymerization of aliphatic polyesters and there is an increasing interest on enzymatically synthesized biopolymers. Synthesis of aliphatic polyesters via enzymatic ring opening polymerization produce polymer without toxicity. Enzyme catalysed polyesters are very convenient for medical and pharmaceutical applications due to their biodegradability and biocompatibility(Bouyahyi et al, 2012).

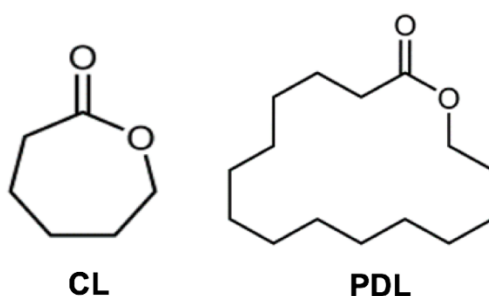


**Figure 2.3 :** Monomers structure of copolymer, from left to right: Caprolactone, Pentadecalactone.

*Candida antarctica* lipase B (CALB) is the most commonly used effective and highly selective enzyme in polymer synthesis(Kundys et al, 2018). Immobilization of enzyme to inorganic and organic surfaces increase their enzyme activity and immobilized

enzymes high temperature resistance(Kundys et al, 2018). Additionally, CALB can easily catalyze esterification and transesterification reactions. Poly (*w*-pentadecalactone-*co*- $\epsilon$ -caprolactone) can be synthesized by ring opening polymerization with immobilized CALB enzymes. Equimolar feed monomer ratio is produced with 97.9% conversion and 20960 g/mol molecular weight value in copolymer(Ulker and Guvenilir, 2018a). Monomers of copolymer has been shown (Figure 2.3), thermal properties of copolymer are improved by Pentadecalactone in copolymer structure(Ulker and Guvenilir, 2018a). Mechanical properties of Poly (*w*-pentadecalactone-*co*- $\epsilon$ -caprolactone) provide advantage when used in drug delivery systems.

## **2.5 Natural Polymers Used in Biomedical Applications**

Nanofibers from natural polymers have been studied in the last decades. Natural polymers include proteins, polysaccharides and nucleic acids(Table 2.3) (Ohkawa et al, 2004). Natural polymer based nanofibers exhibit biocompatible or bio-resorbable properties. One of the widely used natural polymer is chitosan. Chitosan is a cationic polysaccharides, which shows excellent physicochemical properties. These properties are solid state structure and dissolving state conformation(Ohkawa et al, 2004). Chitosan shows not only biocompatibility and biodegradability but also can heals wounds and fights against bacteria and fungi(Geng et al, 2005). Because of these superior properties, chitosan is preferred for spinning alone or as mixture with other polymers. Nanofibers obtained from chitosan are frequently used in drug delivery systems, tissue engineering and wound dressing applications(Geng et al, 2005). Collagen is the most preferred natural polymer for biomedical applications also. Collagen is a part of the extracellular matrix component of tissues(Matthews et al, 2002). Collagen may be used for production of nanofiber to produce biomimetic scaffolds(Rho et al, 2006). Silk is also another important natural polymer. Silk is natural polymer which has fibril protein structure(Ohgo et al, 2003). Silk is produced by silkworm. Fibroin and sericin are the protein parts of silk. Silk exhibits too many excellent advantages for biomedical applications such as good oxygen and water vapor permeability and biodegradability(Min et al, 2004).

**Table 2.3** : Natural polymers and sources(Soares et al, 2018).

<b>Polymer</b>	<b>Source</b>
Chitosan	Shells of crustaceans
Gelatin	Hydrolysis of collagen
Cellulose	Plant fibers and wood
Zein	Corn
Pullulan	Fungal Exopolysaccharide
Alginate	Brown seaweed

## 2.6 Gelatin

Gelatin is a polypeptide which has high molecular weight. It is derived through the acid and alkaline hydrolysis of collagen which is present in animal bones, skin and tendons. It is yellow color powder, water-soluble above 40°C and widely used as gelling agent in food. Gelatin is an irreversibly hydrolyzed form of collagen. Main ingredient of gelatin is protein in structure (Figure 2.4). Polypeptide chain of gelatin includes proline, glycine, hydroxyproline (Table 2.4). There are two types of gelatin, which are Type A and Type B. Gelatin types are defined by pretreatment process. Type A can be treated by acid and Type B can be produce by alkaline pretreatment process. Heating treatment of gel solutions above 40-45°C reduces the viscosity and gel strength(Ranganathan et al, 2019). Strength, water resistance ability and the thermal properties of gelatin nanofibers can be improved by physical or chemical crosslinking. UV irradiation method can be used as physical crosslinking method. Glutaraldehyde vapor is commonly used for chemical crosslinking of gelatin nanofibers(Yang et al, 2018). Due to biocompatibility and biodegradability of gelatin it is a good choice in biomedical, tissue engineering, drug delivery applications(Nguyen and Lee, 2010).

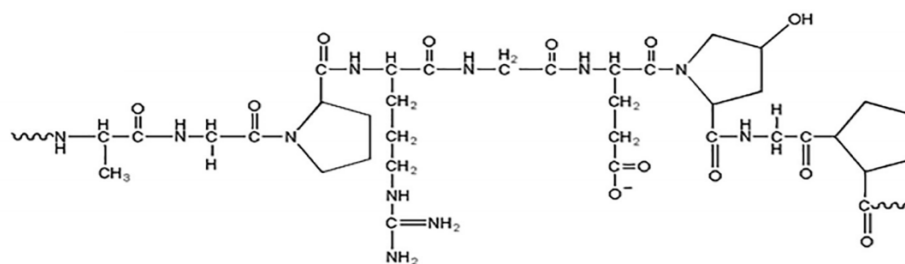


**Figure 2.4 :** Structure of gelatin.

Natural polymers have better biocompatibility than synthetic polymers. However even though gelatin has strong polarity, it has poor fiber formation ability. Gelatin can easily be dissolved in trifluoroethanol and hexafluoroisopropanol (HFIP). Gelatin has amine and carboxylic groups in its structure, this allows to carry a charge by easily ionized in water. This property and hydrogen bonding combination occur limitation to electrospinning process of gelatin(Ko et al, 2010). This limitation can be avoided by mixing gelatin with other synthetic polymers such as PPDL, PCL, PLGA(Huang et al, 2004).

**Table 2.4 :** Amino acids in hydrolysis collagen.

Amino acids	%
Hydroxyproline or prolyne	25
Glycine	20
Glutamic acid	11
Arginine	8
Alanine	8
Other essential amino acids	16
Other non-essential amino acids	12

## 2.7 Solvents for electrospinning process

Selection of suitable solvent for polymers is an important part of electrospinning process. Solubility of solution and electrical conductivity are determined by the solvent. There are two steps in polymer solving, first one is solvent diffusion. Other step is macromolecular chain disentanglement. Solvents may have effect on stability of the process and on morphology of nanofiber.

**Table 2.5 :** Properties of some solvents used in electrospinning.

Solvent	Surface Tension(mN/m)	Dielectric constant	Boiling point(°C)	Density (g/ml)
Acetic acid	22,3	33	64,5	0,791
Formic acid	26,9	6,2	111,8	1,049
Methanol	72,8	80	100	1,000
Chloroform	26,5	4,8	61,6	1,498
Hexafluoro-2-isopropanol	14,7	16,7	59	1,596

The solvent should help sustain the stability of the process. Solvent vapor pressure is an important parameter for evaporation rate and the drying time(Bhardwaj and Kundu, 2010b). Some of the widely used solvents in electrospinning are chloroform, methanol, formic acid and dimethylformamide (DMF) (Table 2.5). Nanofiber size and structure depend on blend viscosity and surface tension(Bhardwaj and Kundu, 2010a). Some studies have shown that, acetic acid and formic acid in binary solvent system have caused finer diameter PCL nanofibers than chloroform solvent system(Van der Schueren et al, 2011). Generally, natural polymers and their blends such as gelatin, collagen, chitosan, cellulose can be solubilized in 1,1,1,2,2,2-hexafluoro-2-propanol (HFIP) or tetrafluoropropanol (TFP)(Xie et al, 2008) (Figure 2.5) . HFIP; which is a fluoro-alcohol solvent, is highly volatile. Hexafluoro-2-propanol is polar and has strong hydrogen bonding properties, which causes substances that serve as hydrogen-bond acceptors to dissolve. Hexafluoro-2-propanol has high density, low viscosity and low refractive index.

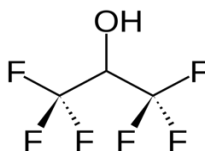


**Figure 2.5 :** Molecular structure of 1,1,1,2,2,2-hexafluoro-2-propanol.

## 2.8 Tetracycline Hydrochloride

Tetracycline is an antibacterial agent which shows activity against gram-positive and gram-negative bacteria (Garrido-Mesa et al, 2013). Tetracycline is effective on preventing skin and bone inflammations from bacterial infection(Chong et al, 2015). Bacterial infections such as acne vulgaris can be treated by tetracycline hydrochloride(Figure 2.6)(Karuppuswamy et al, 2015a).

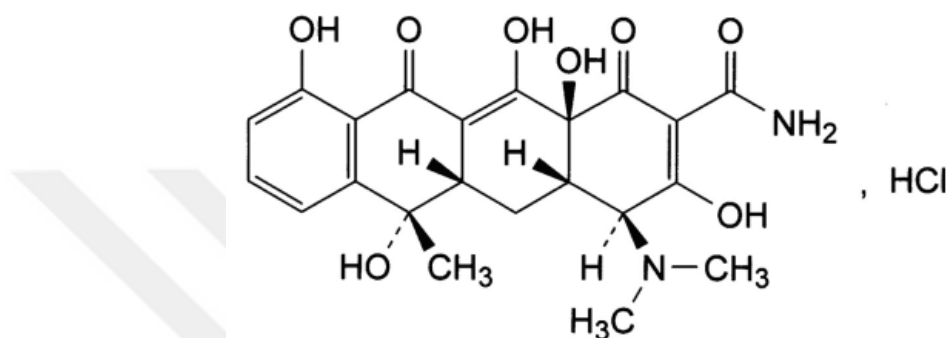


**Figure 2.6 :** Molecular structure of tetracycline hydrochloride.



### 3. MATERIALS AND METHOD

#### 3.1 Materials

Poly( $\omega$ -pentadecalactone-*co*- $\epsilon$ -caprolactone) copolymer, 50%  $\omega$ -pentadecalactone feed weight ratio, was prepared as described in previous studies (Ulker and Guvenilir, 2018b). The free form of the candida antarctica lipase B (CALB, Lipozyme®) was used from Sigma-Aldrich. Rice husk was obtained from a rice production company in Edirne, Turkey. They were washed with distilled water and burned at 600-650 °C for 6 hours to obtain rice husk ashes (RHA). Surface modification of rice husk ashes was achieved with 3-aminopropyl triethoxysilane (3-APTES) (C<sub>9</sub>H<sub>23</sub>NO<sub>3</sub>Si) (Merck). Acetone (Riedelde Häen) (99%, C<sub>3</sub>H<sub>6</sub>O) was used as solvent for 3-APTES. For preparation of pH=7 phosphate buffer, sodium dihydrogen phosphate monohydrate (NaH<sub>2</sub>PO<sub>4</sub>.H<sub>2</sub>O) (Carlo Erba) and disodium hydrogen phosphate heptahydrate (Na<sub>2</sub>HPO<sub>4</sub>.7H<sub>2</sub>O) (Merck) were used. Caprolactone (99%, C<sub>6</sub>H<sub>10</sub>O<sub>2</sub>) (Alfa Aesar) and Pentadecalactone (Sigma Aldrich) were used as monomers of copolymerization. Toluene (99%, C<sub>6</sub>H<sub>5</sub>CH<sub>3</sub>) was used as solvent in the polymerization reaction and was purchased from Merck. In polymerization, chloroform (99%, CHCl<sub>3</sub>) purchased from Sigma Aldrich was used to terminate the reaction, and methanol (99%, CH<sub>3</sub>OH) obtained from Merck was used to precipitate the polymer.

Gelatin was used in blends as natural polymer from bovine (Alfasol). Solvents used for preparation of polymer solutions were; chloroform (Sigma Aldrich, 99.8%), acetic acid (Merck, >99%), formic acid (Merck, ≥99.85%), and 1,1,1,3,3,3-hexafluoroisopropanol (HFIP) (Jinan Finer Chemical Co.). Glutaraldehyde (25% aqueous solution) purchased from Merck was used for cross-linking. For the preparation of 1 L pH 7.4 phosphate buffer saline, 8 g of sodium chloride (Carlo Erba), 0.2 g of potassium chloride (Merck), 1.81 g of disodium hydrogenphosphate dihydrate (J.T. Baker), and 0.24 g of potassium dihydrogen phosphate (Carlo Erba) were dissolved in distilled water. tetracycline hydrochloride (Sigma Aldrich) antibiotic had been used as the active ingredient.

Mueller hinton agar medium (Sigma Aldrich) was chosen and prepared as a medium for testing antibacterial properties.

### 3.2 Method

#### 3.2.1 Enzymatic synthesis of poly( $\omega$ -pentadecalactone-co- $\epsilon$ -caprolactone)

Firstly, home-made biodegradable poly ( $\omega$ -pentadecalactone-co-  $\epsilon$ -caprolactone) was synthesized via enzymatic ring-opening polymerization with 97.9% conversion and 20960 g/mol molecular weight value as described in literature(Ulker and Guvenilir, 2018a).

#### 3.2.2 Preparation of poly(PDL-CL)/gelatin blends

##### Method-1

Primarily, calculated amount of PDL-CL copolymer was dissolved in a Chloroform (CLF): Methanol (MeOH) solvent mixture (3:1, v:v) to achieve 15 wt.% and 30wt.% solutions. Copolymer solutions were stirred for 24 hours at room temperature (Figure 3.1). Thereafter, gelatin was solubilized in a solvent mixture of Acetic Acid(AA): Formic Acid(FA) (1:1, v:v) to obtain 15 wt.% and 8 wt.% solutions. Gelatin solutions were stirred at 40°C for 2 hours. Then, gelatin and copolymer solutions with different wt.% combinations were mixed with various volume ratios (50:50, 70:30) (Table 3.1).

**Table 3.1** : Summary of blends ratio and % concentration for method-1.

S. Number of solution	COPOLYMER		GELATIN	
	Concentration (wt%)	Blend ratio (%)	Concentration (wt%)	Blend ratio(%)
1	15	50	8	50
2	15	50	15	50
3	15	70	8	30
4	15	70	15	30
5	30	70	8	30

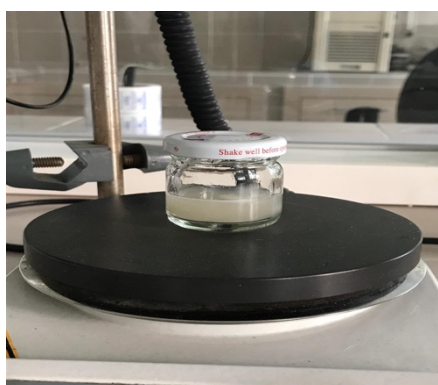


**Figure 3.1** : Blend before electrospinning process.

### Method-2

To start with, calculated amount of PDL-CL copolymer was solubilized in HFIP to obtain 15wt% solution. Solution was stirred for 24 hours at room temperature. During the final 2 hours of stirring process of copolymer, gelatin was solubilized in HFIP in a different flask simultaneously at 40°C to obtain 8wt% solution. Obtained gelatin and copolymer solutions were mixed with varied volume ratios (100:0, 70:30, 60:40, 50:50) ready to be electrospun (Table 3.2).

**Table 3.2** : Summary of blends ratio and % concentration for method-1.

S. Number of solution	COPOLYMER		GELATIN	
	Concentration (wt %)	Blend ratio(%)	Concentration (%wt)	Blend ratio(%)
1	15	100	–	–
2	15	70	8	30
3	15	60	8	40
4	15	50	8	50

### 3.2.3 Electrospinning process of copolymer/gelatin blends

Blends in first and second solvent system were transferred into a 5ml syringe to be delivered via syringe pump with 1.8-2.0 ml/h flow rate. Under 23-25 kV applied voltage electrospinning was performed. Electrospun fibres were collected on a plate covered with aluminium foil, which was placed at a collector 15-17cm away from the

tip and at ambient conditions (Figure 3.2). All electrospinning experiments were conducted on a Nanospinner 24 Touch (Inovenso) electrospinning device.



**Figure 3.2 :** Image of nanofibers after electrospinning.

### **3.2.4 Cross-linking of the most efficient copolymer/gelatin nanofibers**

After electrospinning process, nanofibrous membranes (~0,1mm thickness) were dried in a vacuum oven at 30°C for 24 hours to remove any remaining solvent. Thereafter, 2x2 cm<sup>2</sup> part of nanofibrous membrane was cross-linked under vapour of 25% Glutaraldehyde solution at 25°C for varied time periods (2, 24 hours) in a petri dish. Cross-linked nanofiber membranes were dried in a vacuum oven at 80°C for 2 hours in order to eliminate residual glutaraldehyde from membrane structure.

### **3.3 Preparation of pH 7.4 phosphate buffered saline (PBS) for degradation test**

pH 7.4 Phosphate Buffer was prepared by solubilization of 8 g NaCl, 0,2 g KCl, 1,81 g Na<sub>2</sub>HPO<sub>4</sub>.2H<sub>2</sub>O and 0,24 g KH<sub>2</sub>PO<sub>4</sub> in 1L distilled water. pH of the buffer was controlled by the pH Meter (TWT) and was adjusted to 7.4 by diluted HCl or NaOH.

#### **3.3.1 *In Vitro* degradation tests of cross-linked copolymer/gelatin nanofibrous membranes**

Crosslinked nanofibrous membranes were cut into a size of 1x1 cm<sup>2</sup> parts. Two different methods were applied to test their mechanical properties and solubility resistance. In the first test method, cross-linked (2, 24) and control (without crosslinked) membranes were both soaked into pH 7.4 PBS and kept in vacuum oven at 37°C. Durability of membranes were visually observed daily for ten days. The

second method was mixing membranes and PBS in a tube and placing the membrane PBS mixtures into shaking water bath (JSR, JSSB-Series water bath) at 120 rpm at 37°C (Figure 3.3). The weight loss of membranes were calculated using Equation 1 below.

$$\text{Weight loss(\%)} = \frac{W_o - W_t}{W_o} \times 100 \quad (1)$$

Where  $W_o$  is the initial weight and  $W_t$  is the weight at any time.



**Figure 3.3 :** Water shaking bath for degradation test of membranes.

### **3.3.2 Fabrication of drug loaded copolymer/gelatin nanofibrous membranes**

To begin with, calculated amount of tetracycline hydrochloride; which was arranged to be 0.5, 1, 3, 5 wt.% of total polymer concentration, was dissolved in 10 ml of HFIP. Then, copolymer was added and mixture was stirred for 24 hours at room temperature. The amount of drug included copolymer was adjusted to be 15 wt.% of final solution concentration and calculated amount of gelatin was added and stirred for 2 hours at 40°C. Final concentration of blends were prepared from 8wt.% gelatin and 15wt.% copolymer solutions with 50:50 volume ratio.

### **3.3.3 Electrospinning process of drug loaded copolymer/gelatin nanofibrous membranes**

Drug loaded blends were transferred into a syringe. Mixtures were electrospun with 2ml/h flow rate, 25kV applied voltage, and 17 cm tip to collector distance at ambient conditions (Figure 3.4).



**Figure 3.4 :** Electrospinning Instrument (Inovenso, Nanospinner 24).

### **3.3.4 Cross-linking of drug loaded copolymer/gelatin nanofibrous membranes**

After electrospinning process, drug loaded nanofibrous membranes (0.1mm thickness) were dried at 30°C for 24 hours in vacuum oven in order to remove residual solvent and membranes were cut into 2x2 cm<sup>2</sup> parts. Then, cross-linking was carried out in a desiccator including 10 ml 25% aqueous glutaraldehyde in a petri dish. Drug loaded nanofibrous membranes were cross-linked under glutaraldehyde vapour at 25°C for 2 hours. Cross-linked nanofibers were dried at 80°C for 2 hours for the removal residual glutaraldehyde.

### **3.4 *In vitro* drug release experiments of drug loaded copolymer/gelatin nanofibrous membranes**

Cross-linked tetracycline hydrochloride loaded copolymer/gelatin nanofibrous membranes were cut into 2x2 cm<sup>2</sup> pieces and were weighed. For each drug loading ratio, 3 samples were prepared as defined and were soaked into 10 ml of pH 7.4 phosphate buffered saline (PBS). Then, parts of membranes were placed into shaking water bath at 120 rpm at 37°C. Periodically, aliquots of 1 ml were removed and the removed aliquots were characterized by using UV spectrophotometer (UV 6100S) at 343nm. Removed part of solution was replaced with fresh PBS. The amount of released drug was calculated using the data of the calibration graph (Figure 3.5).

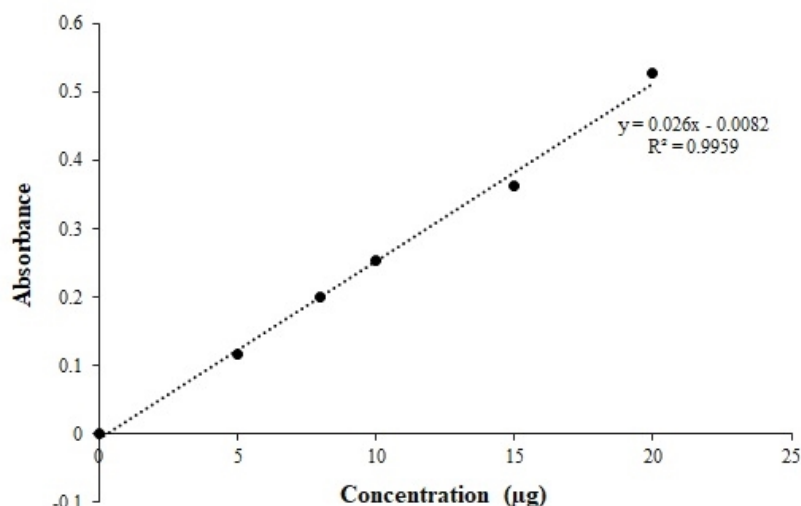


**Figure 3.5 :** Calibration graph of drug release.

Thereafter, cumulative drug release was calculated using Equation 2 Below. (Karuppuswamy et al, 2015b)

$$\text{Cumulative drug release (\%)} = \frac{\text{Total amount of drug released } (\mu\text{g})}{\text{Initial amount of drug present } (\mu\text{g})} \times 100 \quad (2)$$

The calibration graph indicates the absorbance versus concentration values of the free drug in PBS. Amount of cumulative release was determined by adding the amount of drug released from initial time point to any time point. At the time that final measured value was added, total amount of drug released from the membrane was obtained. The initial amount of drug present in the membrane was calculated based on the percentage of drug in the polymer blend and weight of the drug-loaded membrane. (Karuppuswamy et al, 2015b)

### **3.5 Disk diffusion method for observation of antibacterial properties of drug loaded copolymer/gelatin nanofibrous membranes**

#### **3.5.1 Preparation of mueller-hinton agar medium (MHA)**

Mueller-Hinton Agar Medium (MHA) was prepared by solubilization of 38 g Agar in 1L of distilled water. Solution was heated with frequent agitation and was boiled for one minute in microwave oven to completely dissolve the medium. Agar medium was autoclaved at 121°C for 15 minutes to be completely sterilized and was cooled to 40-50°C. Final pH of agar medium had to be  $7.3 \pm 0.1$  at room temperature. Cooled Mueller Hilton Agar was poured into sterile plastic petri dishes on a flat surface to a

uniform depth of 4 mm. Sterile petri dishes were cooled to room temperature and were allowed to solidify. Sterile petri dishes which included agar medium were visually controlled to ensure the absence of water droplets on the surface. Presence of water droplets on the surface of petri dishes, may have resulted in swarming bacterial growth, which could have caused incorrect results. Petri dishes which were not to be immediately used, were stored in the refrigerator inside air tight plastic bags at 2-8°C for up to 4 weeks.

### **3.5.2 Disk diffusion method for investigation of antibacterial properties of membranes**

Antibacterial activity of tetracycline-loaded copolymer/gelatin nanofibrous membranes was investigated by the application of disk diffusion method. Three different bacteria which were *Staphylococcus aureus*, *Bacillus subtilis* as gram positive and *Escherichia coli* as gram negative species, were chosen. Membranes containing different ratio antibiotics and control samples were punched to 6mm diameter by puncher. Firstly, bacteria were incubated in Nutrient Broth at 37°C for 24 h and turbidity of 0.5 Mac Farland was arranged prior to application. Quantity of turbidity was measured by Turbidity Meter. Standardized inoculums had a concentration of  $10^8$  CFU/ml for each type of bacteria. 100  $\mu$ L of bacterial suspension was taken by micropipette and was emptied to petri dishes which contained Mueller Hinton Agar Medium. Bacterial suspension was spread to the surface by cell spreader. Disks were placed to surface of agar petri dishes by the help of blunt forceps. A control disk and three membrane disks containing same ratio of antibiotics were placed to one petri dish. This procedure was repeated for each antibiotic ratio. During this process; the main focus was to prevent the zone to be overlapped therefore 22 mm distance between the disks and 14 mm distanced from the petri edge was kept. Petri dishes were incubated at 37°C for 24 hours in incubator. Inhibition zones of disks were observed and measured after 24 hours.

### 3.6 Characterization Techniques

#### 3.6.1 Scanning electron microscope(SEM) and energy-dispersive X-Ray spectrometer(EDS)

Surface morphology of the copolymer/gelatin and drug loaded copolymer/gelatin membranes were observed by using a scanning electron microscope (SEM, TESCAN VEGA 3). Scannings were operated at 15 kV. Before scanning, membranes were coated with platinum by using a SC7620 sputter coater (Quorum Technologies Ltd, UK). Energy-dispersive X-Ray spectrometer (EDS) connected to SEM was used to evaluate the composition of nanofibers. Diameter of 100 fibers in each SEM image was measured by using Image J software and than mean of the diameters were calculated. For the analysis of fiber diameter distribution, Origin 9.0 software was used.

#### 3.6.2 Ultraviolet (UV) spectrophotometer

The amount of drug released was determined by measuring absorbance on UV mini 1240 SHIMADZU spectrophotometer at 343 nm (Figure 3.6). Solutions containing different drug concentrations were prepared to obtain calibration graph. Phosphate Buffer Solution (PBS) was prepared as blank solution.



**Figure 3.6 :** UV spectrophotometer (UV mini 1240 SHIMADZU).

#### 3.6.3 Fourier transform infrared spectroscopy (FTIR)

Fourier transform infrared spectroscopy (FTIR) analysis was applied on a Perkin Elmer spectrophotometer in order to define the chemical structure of the samples. Each sample was analyzed by KBr pellet. The spectra were recorded by at least 32 scans with a resolution of  $2\text{ cm}^{-1}$ .

#### **3.6.4 Differential scanning calorimetry (DSC)**

Thermal properties were determined by differential scanning calorimetry (DSC) using a TA instruments Q10 calorimeter. Under inert nitrogen atmosphere at a 50ml min<sup>-1</sup> flow rate samples were analysed. Sample scans were carried out between -80 and 200 °C at a rate of 10°C min<sup>-1</sup> with heat-cool-heat thermal cycles and melting temperature (T<sub>m</sub>) and glass transition temperature (T<sub>g</sub>) were measured.

#### **3.6.5 Thermal gravimetric analysis (TGA)**

Thermal gravimetric analysis (TGA) was applied on a Linseis L81 apparatus for thermal characterization of the samples. The samples were heated from 30 to 550°C at a heating rate of 10 °C min<sup>-1</sup> under nitrogen flow.

#### **3.6.6 Water contact angle**

Contact angles of samples were measured by using Attension (KSV) equipment. Water droplets were deposited from a syringe on the surfaces of samples. Static water contact angles were calculated via equipment software. Each sample was measured five times.

## 4. RESULTS AND DISCUSSION

### 4.1 Fabrication of Electrospun Copolymer/Gelatin Nanofibers

As the first solvent system, AA:FA (1:1,v:v) for gelatin and CLF:MeOH (3:1,v:v) for copolymer were chosen. Although a good mixing was applied to the individual solutions as well as the binary mixture, a phase separation was observed in syringe during electrospinning process. As a result of this, occurrence of beaded structures could not be avoided. However, by varying the concentration of polymer solutions and composition of blend, obtaining a nanofiber structure with less defects was possible. Increasing copolymer concentration and/or composition in binary blend resulted in much more beads with few nanofibers between them (Figure 4.1). Also, an increase in gelatin concentration from 8 wt.% to 15 wt.% increased the defects.

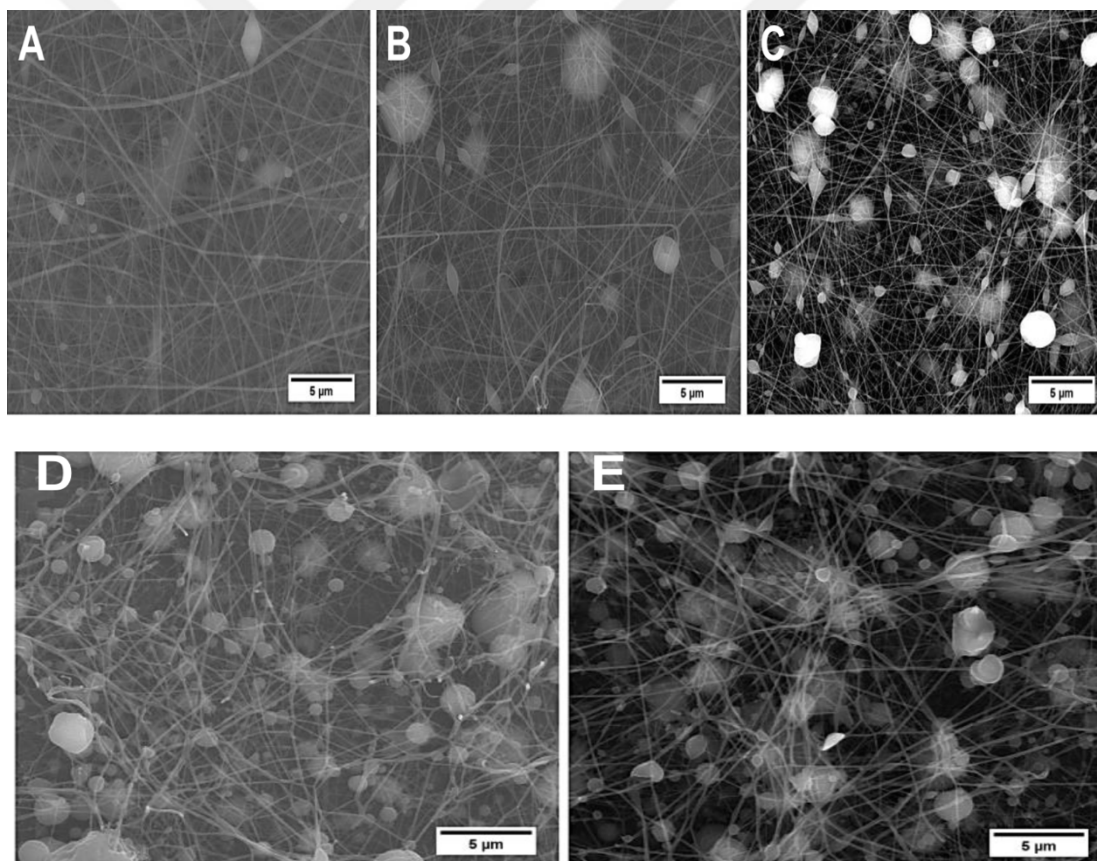


**Figure 4.1 :** Scanner Electron Microscope(SEM) images of 15wt.% copolymer/8wt.% gelatin (50:50) (A), 15wt.% copolymer/15wt.% gelatin (50:50) (B), 15wt.% copolymer/8wt.% gelatin (70:30) (C), 15wt.% copolymer/15wt.% gelatin (70:30) (D), 30 wt.% copolymer/8 wt.% gelatin (70:30) (E) nanofibers.

Diameter distribution of nanofibers showed that, 15 wt.% copolymer and 8 wt.% gelatin concentration with 50:50 (v:v) blending ratio was achieved in well-distributed

nanofibers with  $145.6 \pm 51.9$  nm diameter(Figure 4.2) Even tough phase separation occurred during electrospinning process, still less defects were observed than other samples.

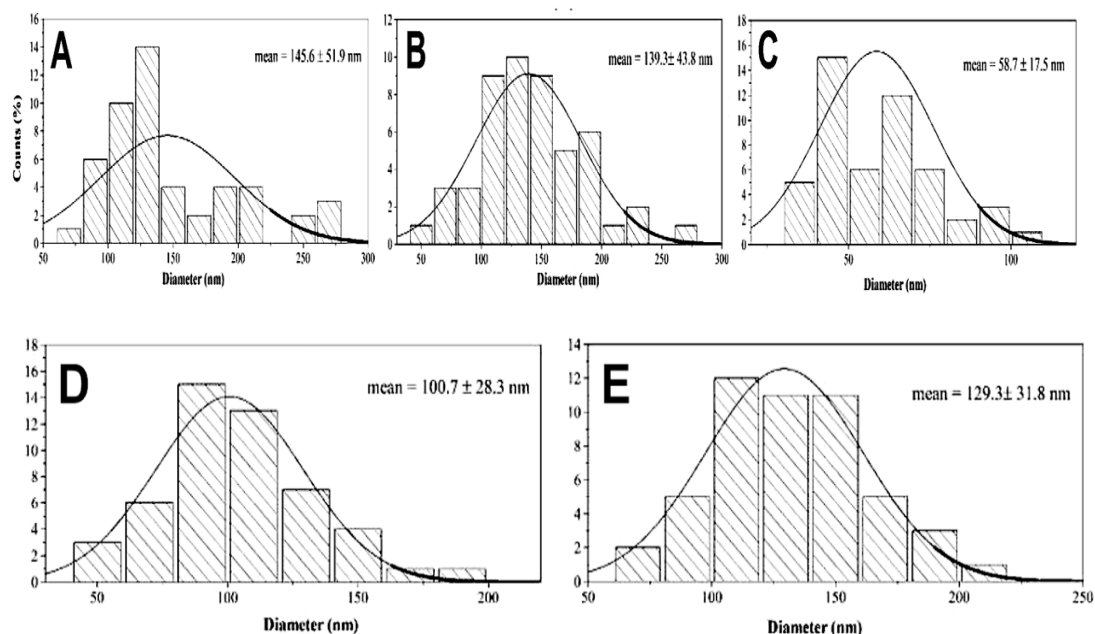


**Figure 4.2 :** Diameter distribution of 15wt.% copolymer/8wt.% gelatin(50:50) (A), 15wt.% copolymer/15wt.% gelatin(50:50) (B), 15wt.% copolymer/8wt.% gelatin (70:30)(C), 15 wt.% copolymer/15wt.% gelatin (70:30)(D), 30wt.% copolymer/8wt.% gelatin (70:30)(E) nanofibers.

In order to avert phase separation, to overcome solubility limitations and to increase the stability in the first solvent system, solvents that could dissolve both copolymer and gelatin were researched and found. Fluorinated alcohol solvents such as hexafluoroisopropanol(HFIP) and trifluoroethanol (TFE) were discovered to be suitable solvents for solving gelatin(Fu et al, 2014)(Choktaweessap et al, 2007). Both copolymer and gelatin were dissolved by HFIP. Both homogenous and transparent blend was successfully achieved by dissolving the copolymer and the gelatin perfectly with the second solvent method(HFIP). SEM images of electrospun nanofibers with varied gelatin compositions showed that increasing the gelatin composition provided smooth nanofibers with well-distributed diameters (Figure 4.3). Equal polymer volume ratio provided best nanofiber morphology (15 wt.% copolymer and 8 wt.% gelatin concentration with 50:50 (v:v). Average fiber diameter of this sample was measured as  $305.0 \pm 45.5$  nm (Figure 4.4). The most efficient copolymer/gelatin nanofibers were crosslinked and drug was loaded.

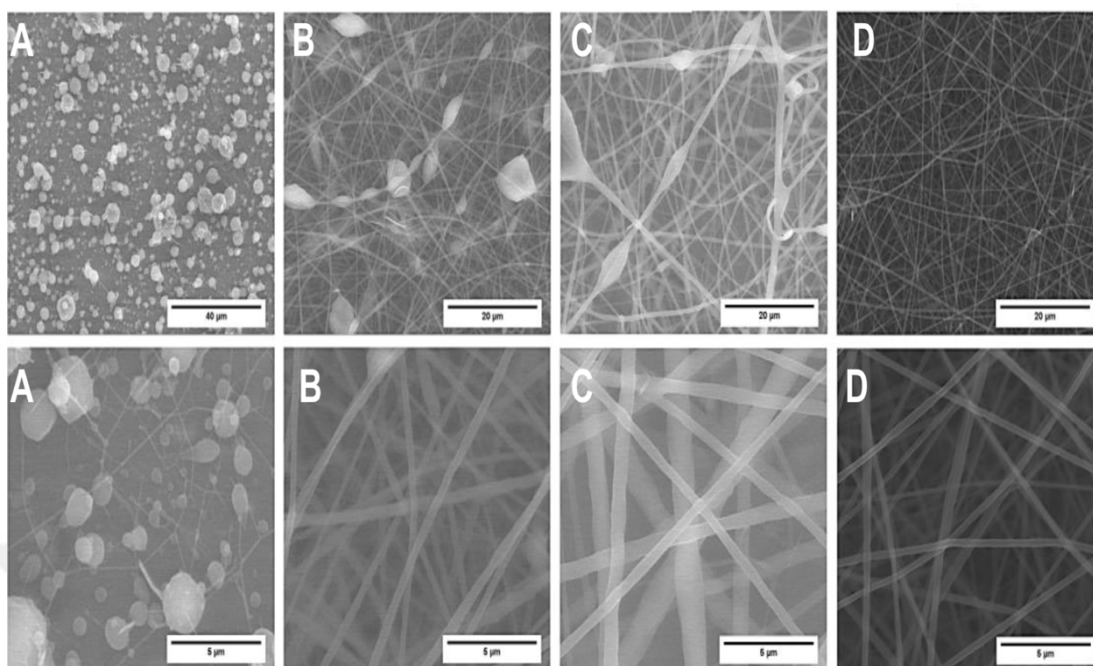


**Figure 4.3 :** SEM images of 15 wt.% copolymer (A), 15 wt.% copolymer/8 wt.% gelatin (70:30) (B), 15 wt.% copolymer /8 wt.% gelatin (60:40) (C), 15 wt.% copolymer /8 wt.% gelatin (50:50) nanofibers (D).

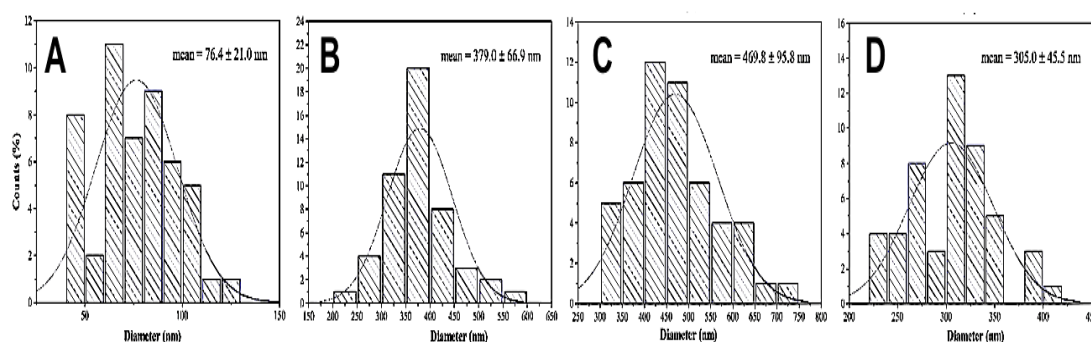
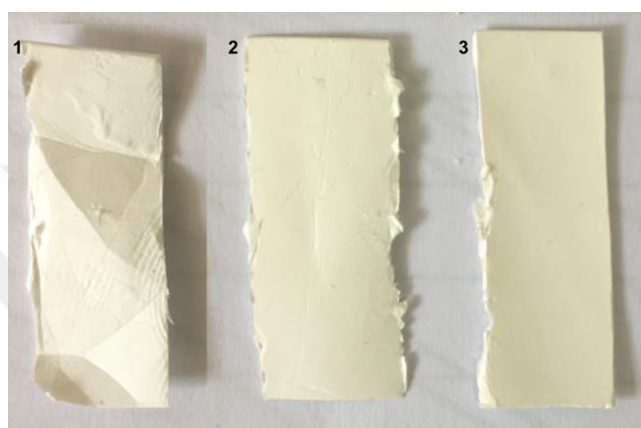


**Figure 4.4 :** Diameter distribution of 15 wt.% copolymer (A), 15 wt.% copolymer/8 wt.% gelatin (70:30) (B), 15 wt.% copolymer/8 wt.% gelatin (60:40) (C), 15 wt.% copolymer/8 wt.% gelatin (50:50) nanofibers (D).

## 4.2 Crosslinking of The Most Efficient Copolymer/Gelatin Nanofibrous Membranes

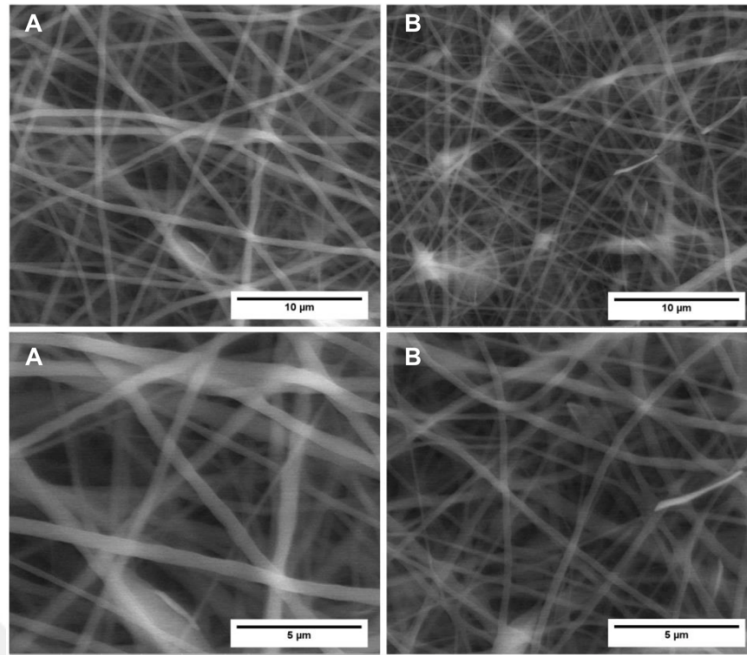
Nanofibrous gelatin has limited application area because it is water-soluble and has mechanically poor properties (Ghasemi-Mobarakeh et al, 2008). In this study, copolymer/gelatin nanofibers were used as drug delivery system. Drug delivery

systems should be stable until the whole drug is released from nanofiber membranes. Consequently, crosslinking was performed to the most efficient copolymer/gelatin nanofibrous membrane. Nanofibrous membrane was crosslinked under the vapour of glutaraldehyde solution for varied time periods (2, 24 hours). In Figure 4.5, various crosslinked samples and control sample was shown. A color change was observed towards yellow for crosslinked samples which may be due to establishment of aldimine (CH=N) linkages between glutaraldehyde and free amine groups of protein during crosslinking(Zhang et al, 2006).

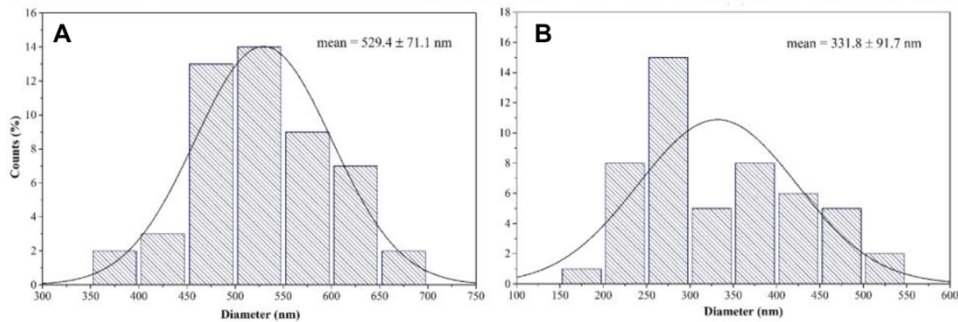


**Figure 4.5 :** Images of non-crosslinked-control (1), 2 hours crosslinked (2), 24 hours crosslinked (3), copolymer/gelatin nanofibrous membrane.

Fiber diameters of the crosslinked membranes were increased compared to the non-crosslinked membranes (average diameter of fiber: ~305 nm). In Figure 4.6; SEM images of 2 hours and 24 hours crosslinked copolymer/gelatin nanofibrous membranes were displayed. As seen, fiber structure of 2 hours crosslinked membranes have better distribution than 24 hours crosslinked membranes (Figure 4.7).



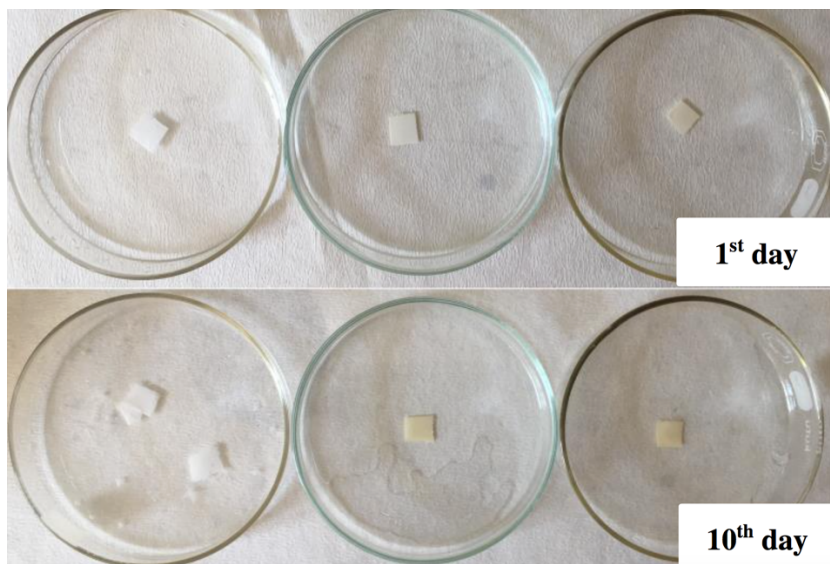
**Figure 4.6 :** SEM images of 2 hours cross-linked (A), 24 hours crosslinked(B), nanofibrous membranes.



**Figure 4.7 :** Diameter distribution of 2 hours cross-linked (A), 24 hours crosslinked(B), nanofibrous membranes.

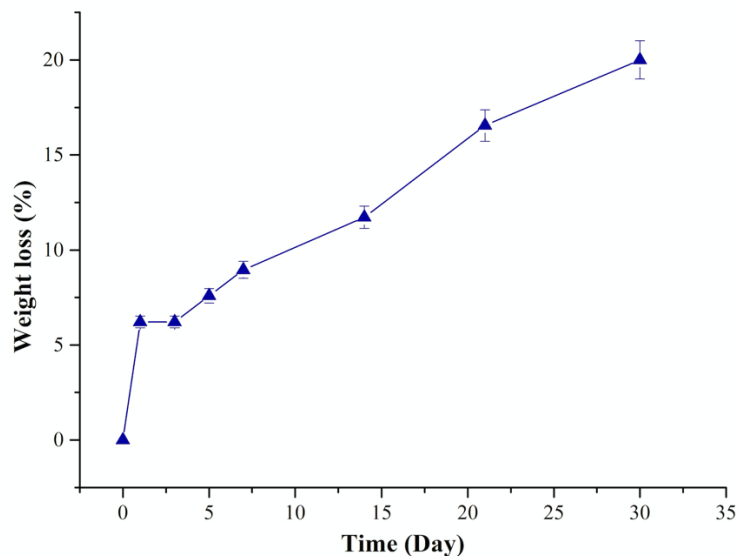
### 4.3 *In vitro* Degradation Test of Cross-linked Copolymer/Gelatin Nanofibrous Membranes

Drug carrying materials should have good mechanical properties in order to efficiently perform controlled and sustained release. Good mechanical strength against human body fluid was awaited to be achieved by crosslinking. Thus, membranes were applied to degradation test. First of all, in order to simulate the human body fluid, non-crosslinked and crosslinked membranes were soaked into pH 7.4 PBS at 37°C (Karuppuswamy et al, 2015b). Crosslinked membranes were stable even at the end of 10 days however non- crosslinked sample was decomposed into pieces (Figure 4.8).

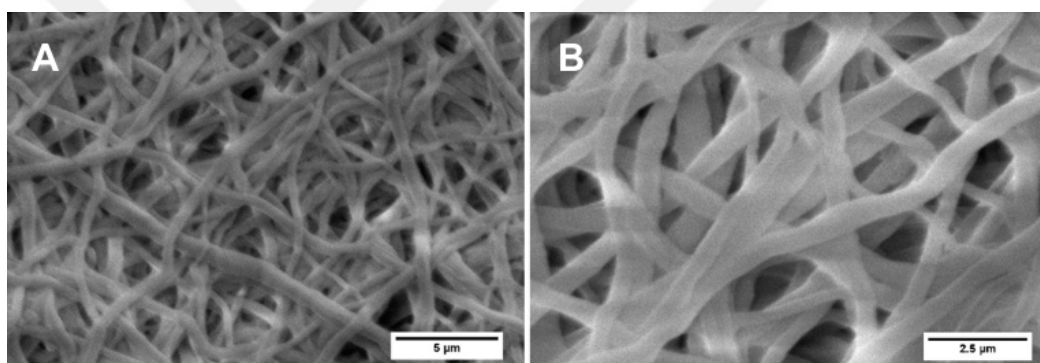


**Figure 4.8 :** From left to right non-crosslinked-control, 2 hours crosslinked, 24 hours crosslinked nanofibrous membranes

Degradation tests showed that, 2 hours crosslinked membrane have good water resistance to PBS. Longer crosslinking process was predicted to ensure high hydrolytic resistance but it may cause toxicity of membranes. Therefore, 2 hours crosslinking was more favourable. It was chosen and further experiments were performed. 2 hours crosslinked membrane was inserted in to PBS buffer and located in shaking water bath. Weight loss was calculated at certain time periods (1, 3, 5, 7, 14, 21, 30<sup>th</sup> days). As seen in Figure 4.9, 20% of initial weight was lost at the end of 10 days. Degradation ratio was higher in the first 2 days, however after 2 days it decelerated. Otherwise, SEM images showed that nanofiber structure was prevented at the end of the 30<sup>th</sup> day of degradation test (Figure 4.10). When compared Figure 4.6A, there was no remarkable change in nanofiber structure.

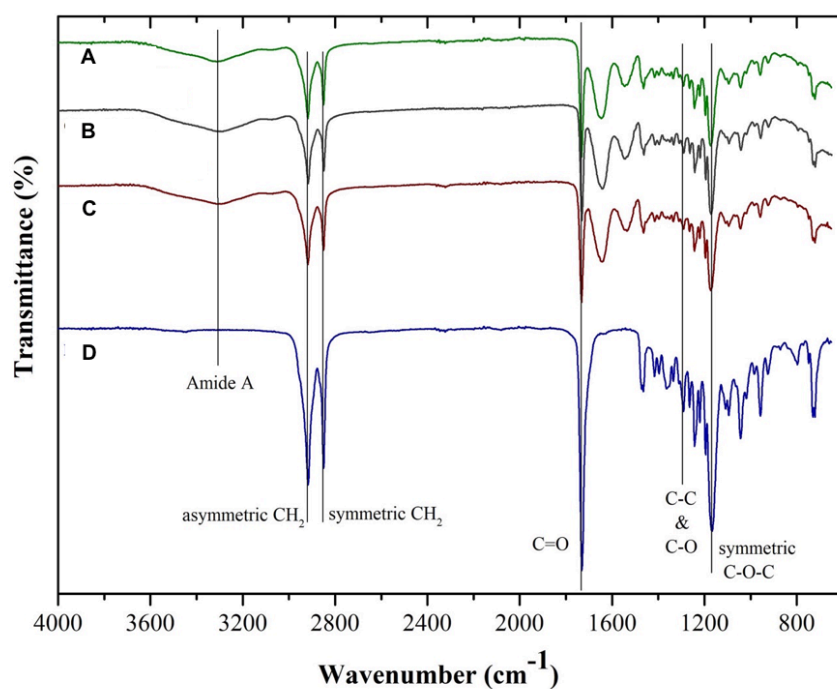


**Figure 4.9 :** Degradation curve of 2hours crosslinked copolymer/gelatin nanofibrous membrane in PBS solution.



**Figure 4.10 :** 2 h cross-linked copolymer/gelatin nanofibrous membrane at the end of 30<sup>th</sup> day of degradation test: (A) 5000x and (B) 10000x magnification.

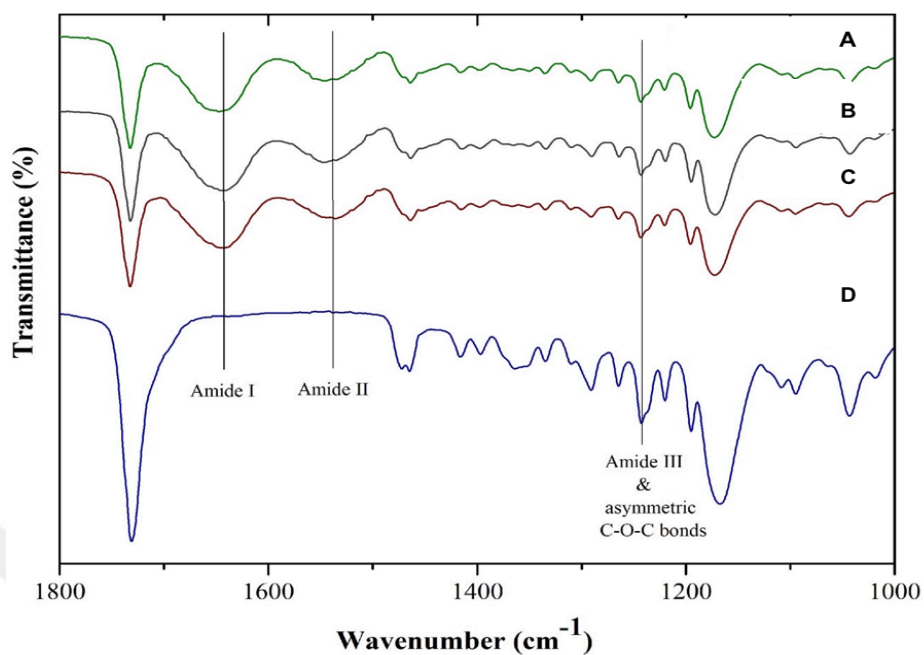
FTIR, water contact angle measurement, DSC and TGA analysis were applied to the most efficient crosslinked and non-crosslinked copolymer/gelatin nanofibrous membranes. Results were compared with copolymer powder. FTIR analysis was also applied to membrane which at the end of 30<sup>th</sup> day of degradation test in order to compare with its initial state (Figure 4.11). As the result of FTIR analysis, there was no change observed in characteristic bands between the two samples.



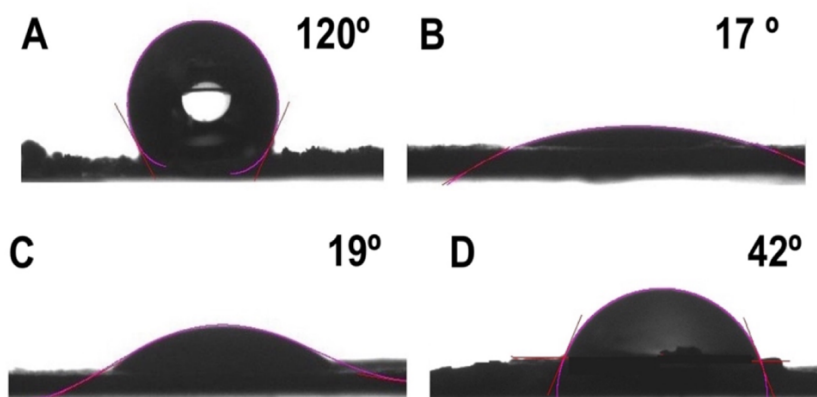
**Figure 4.11** : FTIR spectra of 2h cross-linked copolymer/gelatin nanofiber at its initial state(A) and at the end of 30<sup>th</sup> day(B), copolymer/gelatin nanofiber(C) copolymer powder (D), 4000-600  $\text{cm}^{-1}$ .

Figure 4.11 and Figure 4.12 has shown that, characteristic gelatin peaks occur after blending copolymer solution. Amide A band related to N-H stretching vibration. On the other hand, peak of Amide I corresponding to C-NH bending and C=O stretching. Amide II band belong to C-H stretching and bending vibration of N-H (Zhan et al, 2016)(Nguyen and Lee, 2010). This band was also associated with asymmetric C-O-C bonds of copolymer (H.-K. Wilberth et al, 2015). The peak around  $1450 \text{ cm}^{-1}$  may be related to aldimine linkages that occur after cross-linking (Nguyen and Lee, 2010). All other remarkable peaks were matched to copolymer powder which were compatible with literature (H.-K. Wilberth et al, 2015). As a result of water contact angle measurement (Figure 4.13), Copolymer powder was quite hydrophobic, on the other hand, addition of gelatin provided strong hydrophilic properties as awaited(Liu and Ma, 2009). The drop of water immediately disappeared without maintaining a convex shape on the copolymer/gelatin nanofibres. This showed that copolymer/gelatin nanofibres have better wettability than copolymer and gelatin. Good wettability property of membrane provides an advantage for biomedical applications(Bhattarai et al, 2009). As seen in Figure 4.13, contact angle of nanofiber was increased by crosslinking which proved parallel results as the degradation test

result. These results showed that crosslinked membrane was still hydrophilic, whereas its hydrolytic resistance was increased.



**Figure 4.12 :** FTIR spectra of 2h cross-linked copolymer/gelatin nanofiber at its initial state(A) and at the end of 30<sup>th</sup> day(B), copolymer/gelatin nanofiber(C) copolymer powder (D), 1000-1800 cm<sup>-1</sup>.



**Figure 4.13 :** Water contact angle measurements of copolymer powder (A), copolymer/gelatin nanofiber(B), 2 hours crosslinked copolymer/gelatin nanofiber(C), 24 hours crosslinked copolymer/gelatin nanofiber.

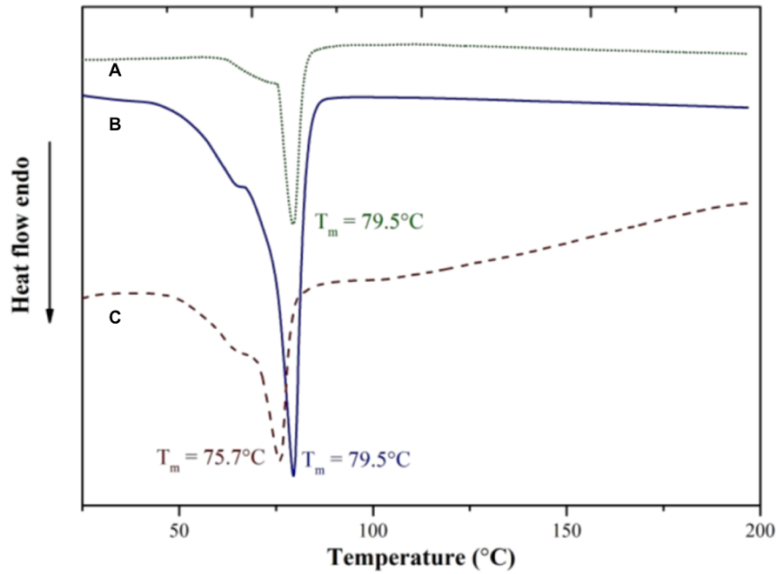


**Figure 4.14 :** Melting temperatures of samples: DSC second heating curves, crosslinked copolymer/gelatin nanofiber (A), copolymer powder (B), copolymer/gelatin nanofiber(C).

Melting temperatures of samples were shown on DSC curves (Figure 4.14). Mixing copolymer with gelatin reduced  $T_m$ , on the other hand after crosslinking of membrane  $T_m$  was increased. Furthermore, Glass-transition temperatures of membranes showed the same behaviour (Figure 4.15, Figure 4.16, Figure 4.17). As a result of increased thermal resistance after crosslinking,  $T_m$  and  $T_g$  values increased.

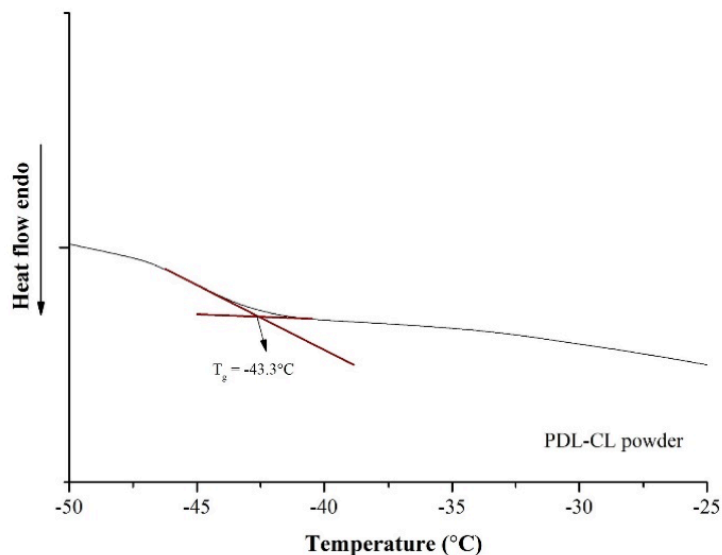


**Figure 4.15 :** DSC second heating curve of copolymer powder, Glass transition temperatures.

By area under melting peaks of copolymer powder, melting enthalpies of copolymer/gelatin nanofiber and crosslinked copolymer/gelatin, were calculated as 104.9, 47.7 and 26.4 J/g, successfully.

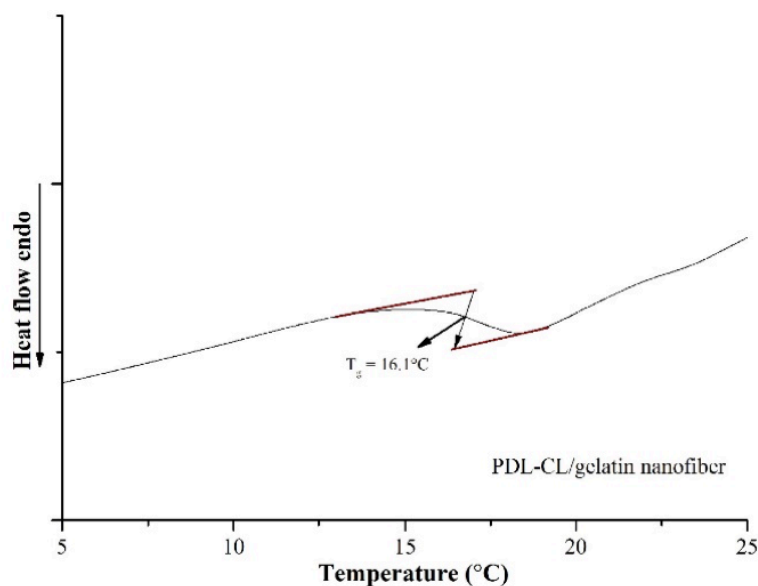


**Figure 4.16 :** DSC second heating curve of copolymer/gelatin nanofiber, Glass transition temperature.

Gelatin and copolymer melting endotherms were appeared in the same range, furthermore, results presented important decrease in melting enthalpy by the addition of gelatin as expected (Kasapis and Sablani, 2005).

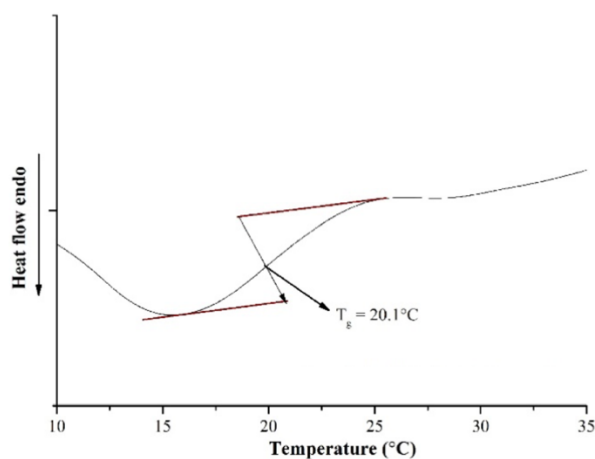


**Figure 4.17 :** DSC second heating curve of 2 h cross-linked copolymer/gelatin nanofiber: Glass transition temperature.

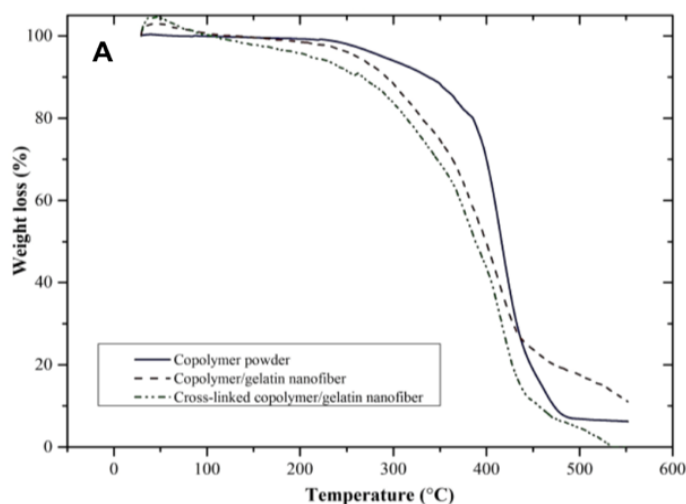


**Figure 4.18 :** TGA results of copolmer powder, copolymer/gelatin nanofiber, and 2 h crosslinked copolymer/gelatin nanofiber: weight loss (A).

As a result of TGA, copolymer powder had a single degradation temperature at 419.2°C, however copolymer/gelatin nanofiber had three step degradation (Figure 4.18, Figure 4.19). The first degradation temperature (75.6°C) belonged to solvent/water evaporation. Second degradation pattern was disappeared after cross-linking which proved the increase of thermal properties after cross-linking. Main degradation was observed at 404.4°C which was lower than poly(PDL-CL) powder.

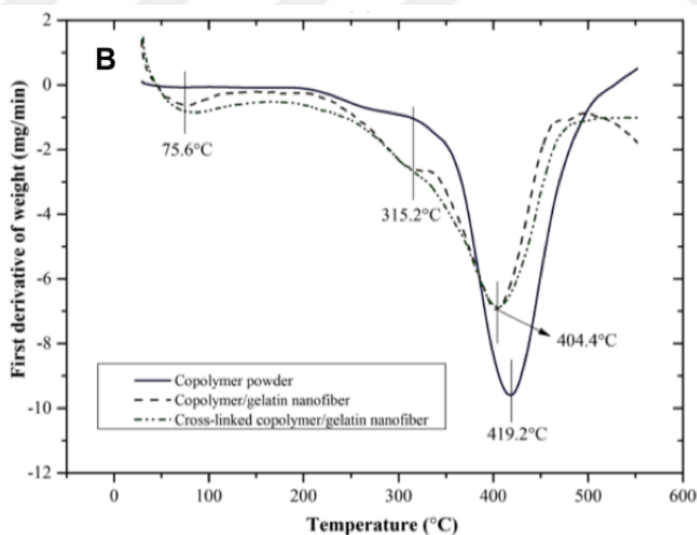


**Figure 4.19 :** TGA results of copolmer powder, copolymer/gelatin nanofiber, and 2 h crosslinked copolymer/gelatin nanofiber: (B) first derivative of weight.

#### **4.4 Fabrication of Drug Loaded Electrospun Copolymer/Gelatin Nanofiber Membranes**

In the first part of this study; suitable solvent systems for copolymer/gelatin blends in electrospinning process, copolymer-gelatin concentrations and binary blend ratios has been investigated. As a second part of study, varied amounts (0.5, 1, 3, and 5%) of tetracycline hydrochloride antibiotic was added to optimum copolymer/gelatin blend (copolymer 15 wt.% and gelatin 8 wt.% concentrations, blend ratio (50:50, v:v), as a most suitable solvent: HFIP) electrospun in optimum conditions previously discovered in this study. SEM images of varied amount of drug loaded nanofibers showed that, both samples had smooth and regular structure without beads and defaults (Figure 4.20). In general, Normal fiber diameter distribution was obtained. In addition to this, a few nanofiber forms were larger in diameter. Orientation of two nanofibers on top of each other may have caused these larger fibers. Consequently, standard deviations of nanofiber diameters increased.

An average diameter of copolymer/gelatin nanofibers was found  $298.3 \pm 82.4$  nm at first step of the studies (Figure 4.7). After drug loading process, diameter of nanofibers decreased. At the lowest drug loading ratio (0.5 wt.%), highest average nanofiber diameter ( $282.9 \pm 64.6$  nm) was measured. Other drug loading ratios (1, 3, and 5 wt.%) caused formation of thinner nanofibers (180-200 nm) ( $p < 0.001$ ). However, there were no notable diameter difference among these three drug-loaded nanofiber membranes ( $p > 0.05$ ). After crosslinking process, structure of fibers were preserved with remarkably increased fiber diameters ( $p < 0.001$  or  $p < 0.05$ ) (Figure. 4.20). On the other hand, average diameter was still small enough (215-350 nm). Afterwards, to identify the presence of tetracycline hydrochloride in the structure of membrane, EDS spectrum of 0.5 wt.% drug loaded and cross-linked nanofiber was analyzed. Chloride(Cl) existed in the molecular structure of tetracycline hydrochloride(Garrido-Mesa et al, 2013). Since chloride peak appeared, the presence of antibiotics in the structure of the membrane was proven (Figure 4.20F). In addition to the results, Sulphur(S) and Nitrogen(N) peaks were defined in EDS spectrum that confirmed the existence of gelatin in the nanofibers membrane(Chong et al, 2015)(Tonda-Turo et al, 2018).

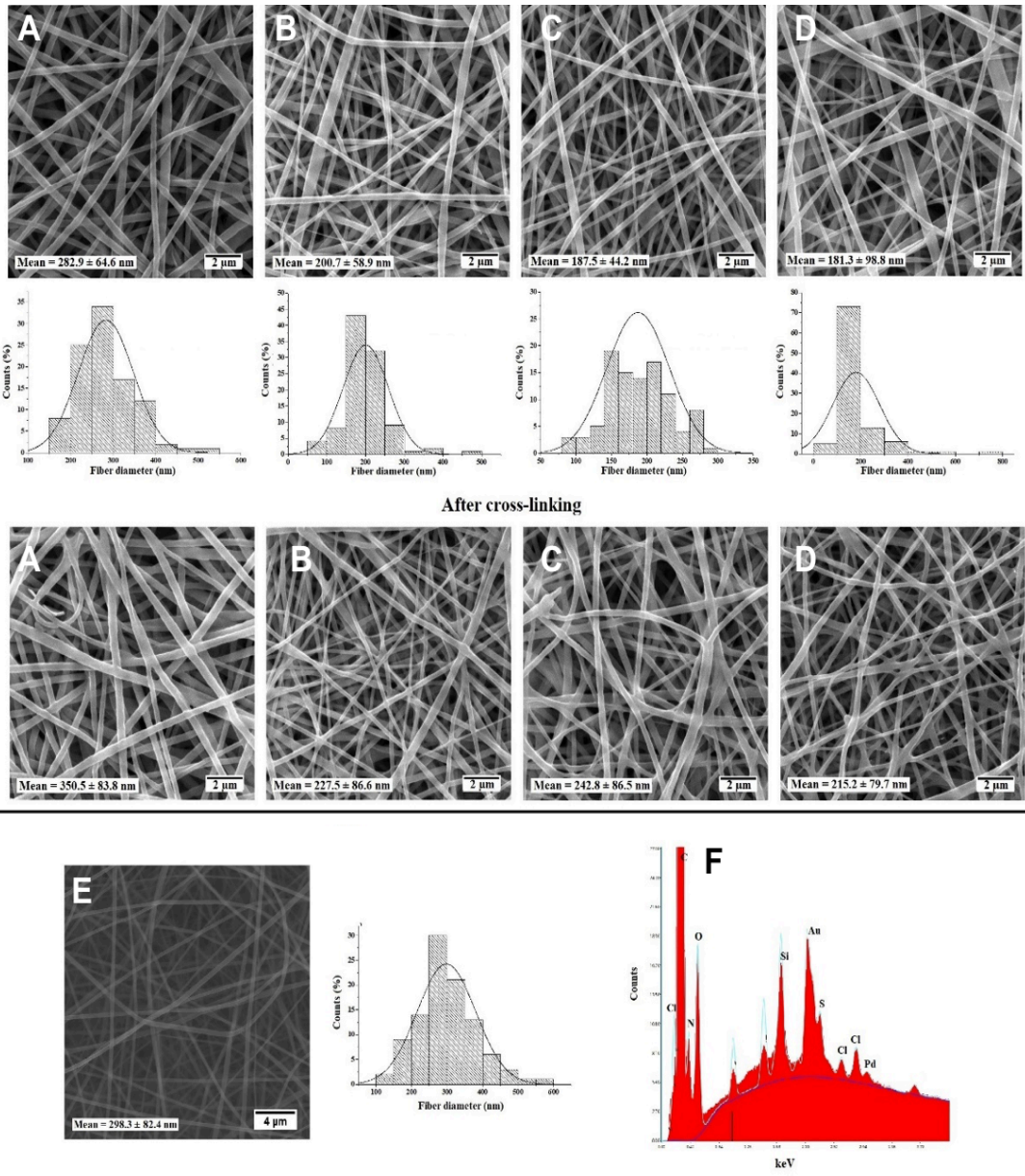


**Figure 4.20 :** SEM images of drug loaded copolymer/gelatin nanofibrous membranes before and after cross-linking: 0.5(A), 1(B), 3(C), 5(D) wt.% tetracycline loading ratios, copolymer/gelatin nanofiber(E), EDS analysis of 0.5 wt.% drug loaded and cross-linked nanofibrous membrane(F).

#### 4.5 *in vitro* Drug Release Studies of Copolymer/Gelatin Nanofibrous Membrane

In the previous periods of the study, varied amounts of tetracycline hydrochloride loaded copolymer/gelatin nanofiber membranes were formed, successfully. As the next step of the study, Drug release behaviors of membranes were examined. In Figure 4.21, cumulative drug release with time for each drug ratio was shown.

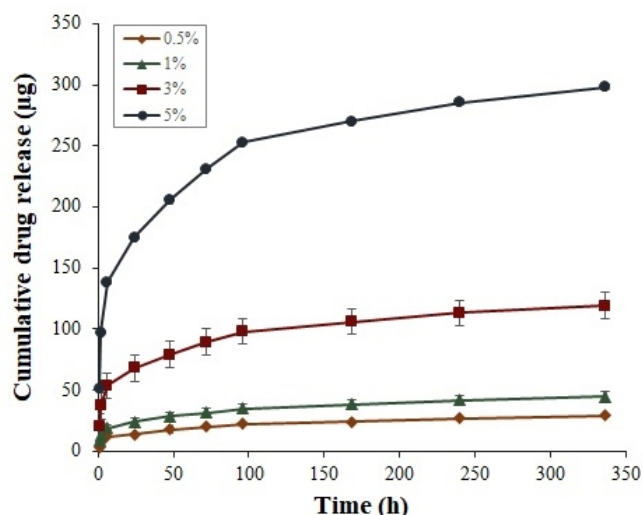


**Figure 4.21 :** Drug release graph of drug loaded copolymer/gelatin nanofibrous membrane

Figure 4.21 showed that, drug release behaviour was parallel with an initial fast release and gradual release until 14<sup>th</sup> day. As seen in the Table 4.1, Initial burst release was less than 11% for all drug rates in 1 hour. Additionally, 5 wt.% drug loaded membrane had the lowest burst release percentage ( $8.2 \pm 0.1$  %). On the other hand, total drug release percentage of 5wt.% was the lowest ( $48.1 \pm 0.7$  %). SEM images of 5wt.% showed that there were some thicker fibers in formation of membrane. These fibers may have hindered the drug diffusion. However, 0.5 wt.% drug loaded membrane performed remarkably the highest total drug release percentage ( $69.4 \pm 0.2$  %) with relatively low initial burst release percentage ( $9.1 \pm 0.1$  %).

**Table 4.1 :** Result of antibiotic release.

Amount of drug (%)	Burst release within 1 h (%)	Total drug release (%)
<b>0.5</b>	<b><math>9.1 \pm 0.1</math></b>	<b><math>69.4 \pm 0.2</math></b>
<b>1</b>	<b><math>10.5 \pm 1.1</math></b>	<b><math>55.6 \pm 4.3</math></b>
<b>3</b>	<b><math>9.7 \pm 0.3</math></b>	<b><math>57.9 \pm 1.9</math></b>
<b>5</b>	<b><math>8.2 \pm 0.1</math></b>	<b><math>48.1 \pm 0.7</math></b>

Drug loaded membranes were dried and scanned by SEM after the end of 14-days drug release. In Figure 4.22, both nanofibrous structures were disrupted as a result of

drug release. Moreover, the morphologies seemed to be uniform which may be a result of uniformly loaded and released drug.

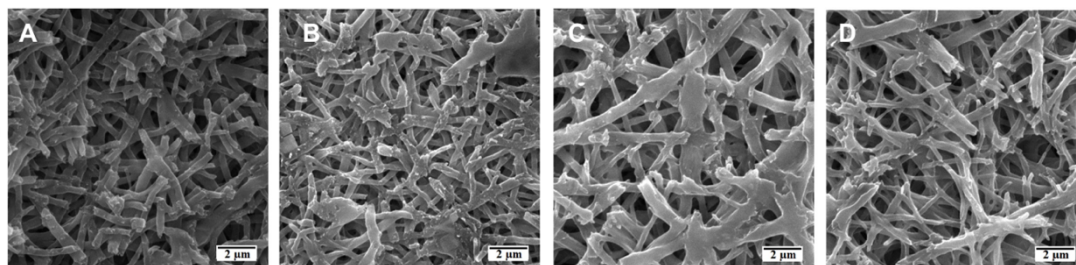


**Figure 4.22** : SEM images obtained at the end of 14-days drug release: (a) 0.5, (b) 1, (c) 3, (d) 5 wt.% tetracycline loading.

#### 4.6 Antibacterial Activity Tests for Drug Loaded Copolymer/Gelatin Nanofibers

Antibacterial activity of drug loaded copolymer/gelatin membranes was investigated by measuring the zone of growth inhibition (Balouiri et al, 2016). Antibacterial activities were tested against Gram-positive (*S. aureus* and *B. subtilis*) and Gram negative (*E. coli*) bacteria. Figure 4.23 and Figure 4.24 display the inhibition zones and their diameters, respectively. The results showed that, all samples with varied antibiotic loading ratios exhibited clear inhibition zones against Gram positive bacteria *S. aureus* and *B. subtilis*. Larger inhibition zones (~30-40 mm) were observed in *B. subtilis* petri dishes which indicated that drug-loaded preparations were extremely active against this bacterium. However, samples were not as effective against *E. coli*. For 0.5 wt.% tetracycline hydrochloride ratio, no inhibition zone was detected and higher concentration samples displayed limited antibacterial activity (~8-10 mm inhibition zone). Consistent with the literature, Gram negative bacterium *E. coli* was found to be more resistant to antibiotic. This antibiotic resistance may have originated from double-membraned structure of Gram negative bacteria in which the external membrane was responsible for immune response. Gene-level studies had also shown that, *E. coli* strains had genes that were responsible for resistance to tetracycline (Karami et al, 2006). Additionally, inhibition zones were expanded with increased antibiotic concentration as expected.

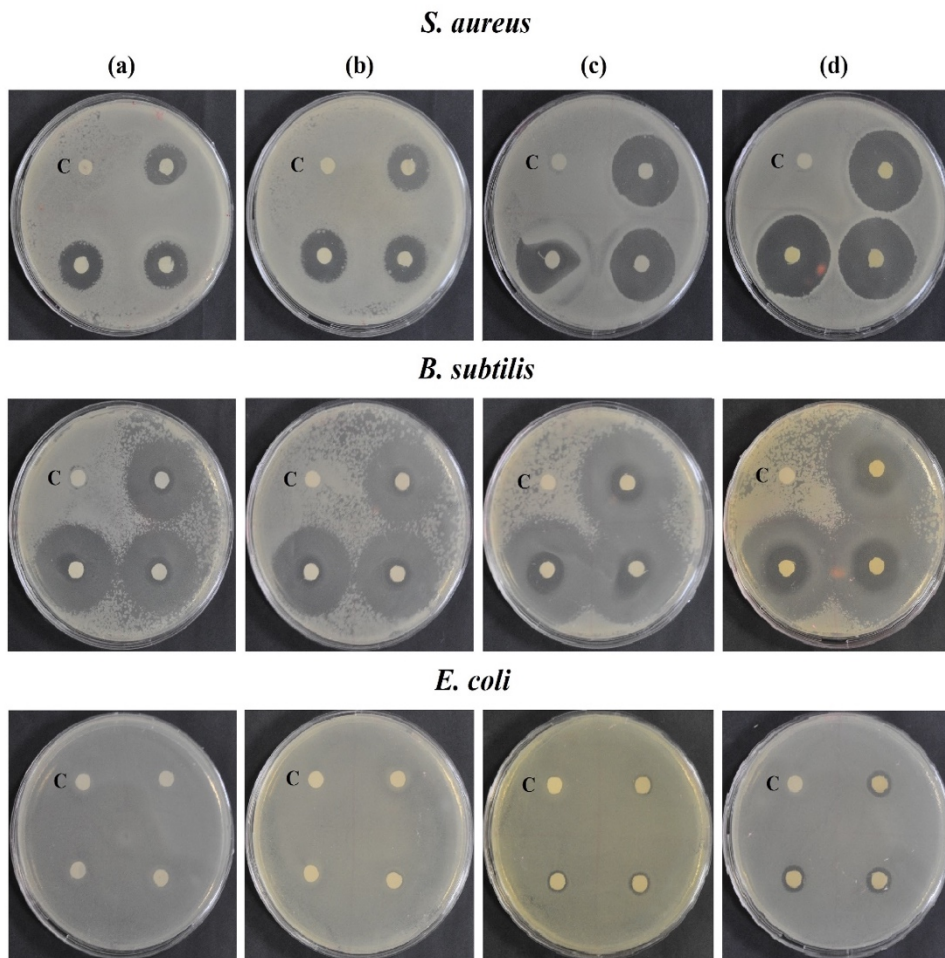


**Figure 4.23 :** Antibacterial activities of (a) 0.5, (b) 1, (c) 3, and (d) 5 wt. % antibiotic loaded samples against *S. aureus*, *B. subtilis*, and *E. coli*. (Each petri dish includes a control and three replicate disks.)

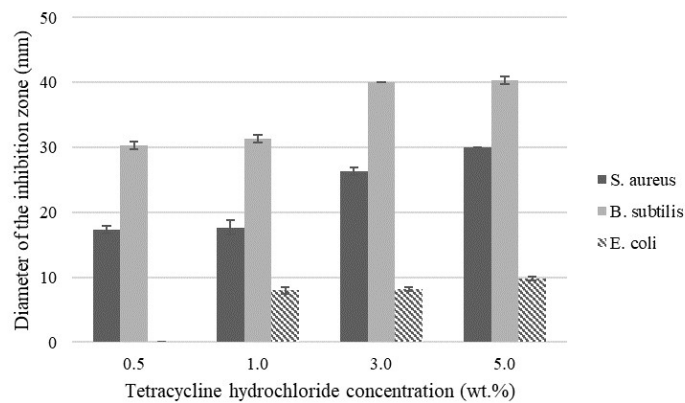


**Figure 4.24 :** Comparison of diameter of inhibition zones.

#### 4.7 FTIR Results of 0.5% Drug Loaded Copolymer/Gelatin Nanofibers

FTIR spectra of cross-linked neat and drug-loaded copolymer/gelatin nanofibrous membranes were compared (Figure 4.25). Characteristic gelatin and copolymer bands were detected in both two spectra and labeled on the figure. Briefly, observed typical gelatin bands were; amide A band associated with N-H stretching vibration, amide I band belonged to C=O stretching and C-NH bending, amide II band demonstrated bending vibration of N-H group and C-H stretching, and amide III band belonged to bending vibration of C-N group (Nguyen and Lee, 2010). Amide III band was also associated with asymmetric C-O-C bonds of copolymer (H. K. Wilberth et al, 2015). All other marked peaks were belonged to copolymer powder which were compatible with literature (H. K. Wilberth et al, 2015). In order to interpret the establishment of drug molecule, it is necessary to discover its molecular structure. Tetracycline hydrochloride has three functional groups which are tricarbonylamide, phenolic diketone, and dimethylamino. Tricarbonylamide, which was shown as A ring in Figure 7(c), is the most characteristic region and observed between  $1700\text{-}1500\text{ cm}^{-1}$ . Tricarbonylamide consists of an amide and two independent carbonyls (Myers et al, 1983). Figure 7(b) presents  $1700\text{-}1500\text{ cm}^{-1}$  part of the spectra in which two peaks were detected at  $1645\text{ cm}^{-1}$  (amide I) and  $1540\text{ cm}^{-1}$  (amide II) (Li et al, 2010; Myers et al, 1983). These bands were common for both neat and drug-loaded samples, since characteristic gelatin and TCH bands were overlapped.

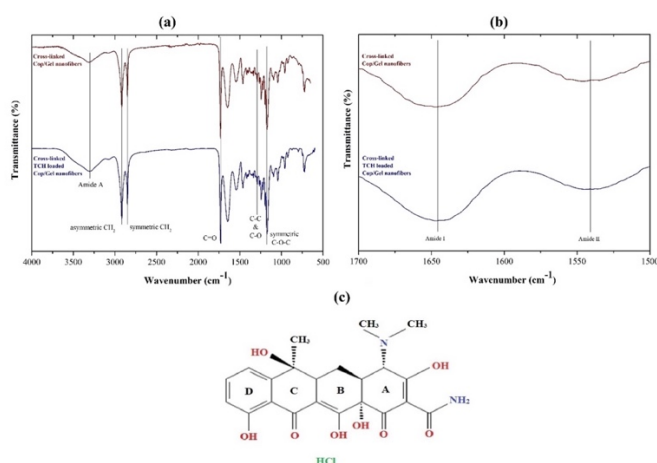


**Figure 4.25 :** FTIR spectra of cross-linked copolymer/gelatin and cross-linked TCH loaded copolymer/gelatin nanofibers (a) full spectra, (b) spectra between  $1700\text{-}1500\text{ cm}^{-1}$  and (c) molecular structure of TCH.

#### 4.8 DSC Results of 0.5% Drug Loaded Copolymer/Gelatin Nanofibers

In order to understand the physical state of the drug in the electrospun nanofibers, which is crucial for attaining desired drug release profiles, DSC analysis were applied to cross-linked neat and drug-loaded copolymer/gelatin nanofibrous membranes. It is known from literature that, the DSC thermogram of TCH has an endothermic melting peak at 220.9°C (Cervini, Machado, et al, 2016). As seen from Figure 4.26, cross-linked neat copolymer/gelatin nanofibers showed a single melting endotherm at 79.5°C. Drug-loaded preparation exhibited a similar melting phenomenon at 78.3°C, however the melting peak of TCH was absent. This situation was familiar with some other drug-loaded electrospun matrices in literature such as; metronidazole benzoate loaded polycaprolactone, diclofenac sodium loaded Eudragit® L 100-55, teriflunomide loaded polylactic acid/polybutylene adipate, and naproxen loaded cellulose acetate nanofibers. It was hypothesized that the absence of melting endotherms of drugs in drug-loaded nanofibers was a result of dispersion of drug molecules in amorphous state within the nanofibers without formation of drug crystals. In the present study, the slight lowering of the melting point ( $T_m$ ) after TCH loading indicated a reduction of crystallinity (He et al, 2017; Zamani et al, 2010). Additionally, DSC curve of TCH-loaded sample gave rise to a broad endothermic event around 125°C which may be related with the release of small amount of water adsorbed on the sample (Cervini, MacHado, et al, 2016).

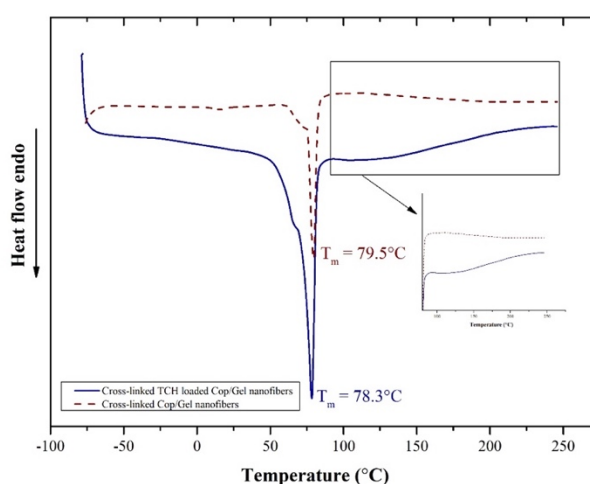


**Figure 4.26 :** DSC results of cross-linked neat and TCH-loaded copolymer/gelatin nanofibers.

#### 4.9 TGA Results of 0.5% Drug Loaded Copolymer/Gelatin Nanofibers

TGA weight loss (TG) and first derivative of weight loss (DTG) curves of cross-linked neat and drug-loaded copolymer/gelatin nanofibrous membranes exhibited mass losses in two or three consecutive steps (Figure 4.27). First mass loss (~7.6%) was common for both neat and drug-loaded samples and related with solvent/moisture evaporation. TG and DTG curves of drug-loaded sample showed a degradation pattern around 316.9°C with mass loss of 30.2%. This pattern was missing in TGA curves of neat sample, therefore it would be related with thermal decomposition of TCH molecule. Main degradations (~56.8% mass loss), which resulted from thermal decomposition of polymeric structure, were observed at 406°C and 415.1°C for neat and drug-loaded nanofibrous membranes, respectively.

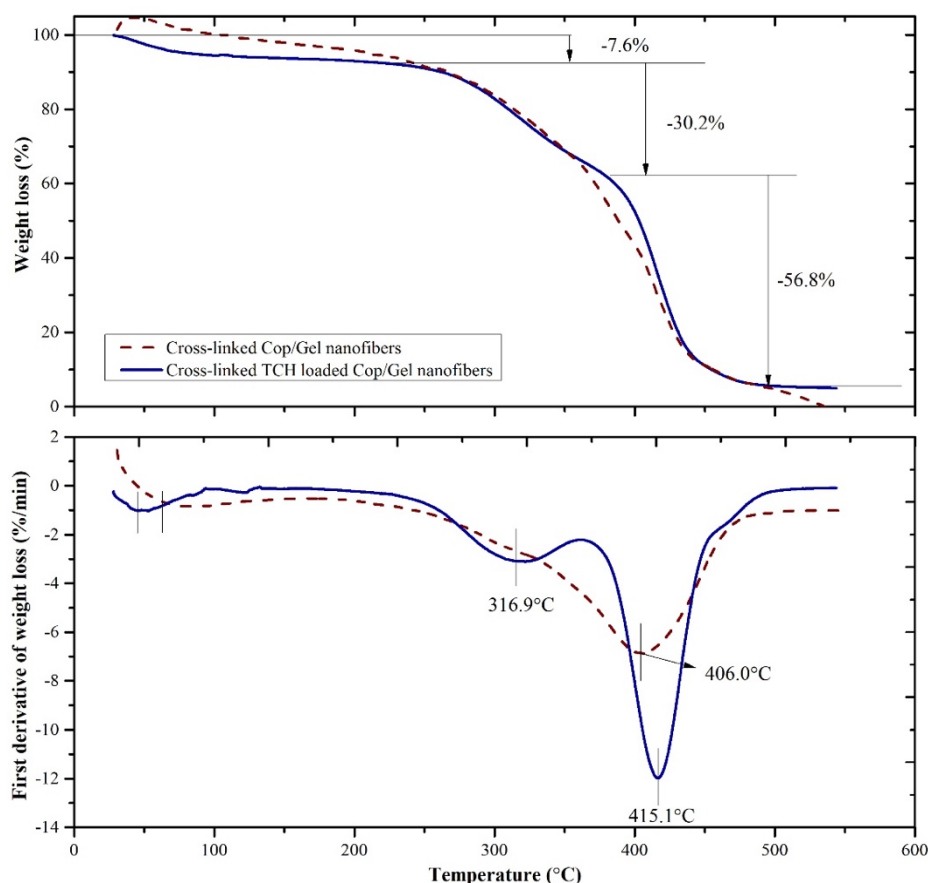


**Figure 4.27 :** TGA results of cross-linked neat and TCH-loaded copolymer/gelatin nanofibers.

## 5. CONCLUSIONS AND RECOMMENDATIONS

In this study there are two parts. First part is the determination of solvent systems and copolymer/gelatin concentration rate in blend to fabricate copolymer/gelatin nanofiber in success. Second part of study is; loading drug to most efficient membrane and investigation of drug release behaviour of copolymer/gelatin nanofiber membrane. Firstly, Poly(*w*-pentadecalactone-*co*-*e*-caprolactone) was selected as home-made copolymer and it was synthesized as described in the previous studies(Ulker and Guvenilir, 2018b). AA:FA(1:1,v:v) for gelatin and CLF:MeOH(3:1,v:v) for copolymer was determined as the first solvent system. Clean mixture was established during mixing by solubilizing gelatin in AA:FA and copolymer in CLF:MeOH. However, during blending of copolymer and gelatin solutions; although it looked clean for a while, phase separation occurred in syringe during process. The reason of phase separation was incompatibility between four solvents used in the blend system. On the other hand, concentration rate was changed in binary blend system. 15 wt.% copolymer and 8 wt.% gelatin concentration with 50:50 (v:v) blending ratio was achieved in well-distributed nanofibers. It was proven by SEM images but phase separation could not be prevented due to solvent incompatibilities.

As a result of the literature research, HFIP was discovered to be the most successful solvent for both copolymer and gelatin. Both homogenous and transparent blend was successfully achieved by using HFIP. During electrospinning process, phase separation did not occur. SEM images showed that 15 wt.% copolymer 8 wt.% gelatin (50:50, v:v) blend provided well distributed and finer diameter nanofibers. Due to this, 15 wt.% copolymer 8wt.% gelatin (50:50, v:v) was selected for the later stages of the studies. Cross-linking, degradation tests, characterization, and drug loading were applied to this sample.

As the next step of the study, nanofibrous membrane was crosslinked under the vapour of glutaraldehyde solution for varied time periods (2, 6, 24, 30 hours), successfully. Degradation tests showed that 2 hours of crosslinking process improved mechanical properties of membranes. Moreover, fiber diameters of the crosslinked membranes increased compared to the non-crosslinked membranes. As seen in SEM images, 2 hours crosslinked membranes had better distribution than 24 hours crosslinked membranes. Non-Crosslinked and crosslinked membranes were soaked into pH 7.4

PBS at 37°C to determine hydrolytic resistance of membranes. Degradation results showed that 2 hours of crosslinking was enough to increase hydrolytic resistance without reducing hydrophilicity. At the end of 30<sup>th</sup> day, nanofiber structure of membrane was prevented.

Results of copolymer/gelatin FTIR analysis showed that, characteristic gelatin peaks occur after blending copolymer solution. Amide A band related to N-H stretching vibration. On the other hand, peak of Amide I corresponding to C-NH bending and C=O stretching. Amide II band belong to C-H stretching and bending vibration of N-H (Zhan et al, 2016)(Nguyen and Lee, 2010). This band was also associated with asymmetric C-O-C bonds of copolymer (H.-K. Wilberth et al, 2015). The peak around 1450 cm<sup>-1</sup> may be related to aldimine linkages that occur after cross-linking (Nguyen and Lee, 2010). All other remarkable peaks were matched to copolymer powder which were compatible with literature (H.-K. Wilberth et al, 2015).

Hydrophilic properties of copolymer/gelatin membrane were examined. Water contact angle analysis showed that, addition of gelatin increased hydrophilic properties as awaited. According to the test results, copolymer/gelatin nanofiber was more hydrophilic than copolymer and gelatin. However, crosslinking process increased the contact angle of membrane, as expected. After crosslinking, even though water resistance of membranes improved membrane were still hydrophilic. Good wettability of membrane made the membrane a strong candidate for drug delivery device.

Thermal behaviour of copolymer powder, copolymer/gelatin nanofiber and 2h crosslinked copolymer/gelatin nanofiber were successfully investigated by TGA and DSC. As seen in DSC results, T<sub>m</sub> and T<sub>g</sub> was decreased by blending copolymer with gelatin. Crosslinking process increased T<sub>m</sub> and T<sub>g</sub>. According to these results, thermal resistance of membrane was improved by crosslinking. As per TGA results, curve of copolymer powder showed single degradation temperature at 419.2°C. Copolymer/gelatin nanofiber had three step degradation; two of which were; solvent/water evaporation at 75.6°C, main degradation at 404.4°C and as the third step, second degradation curve disappeared after crosslinking. That was the proof for improvements of thermal properties after crosslinking process.

In this work, varied amounts (0.5, 1, 3, and 5%) of tetracycline hydrochloride antibiotic loaded copolymer/gelatin nanofibers were fabricated successfully. SEM images

showed that, there were no beads and defects in nanofiber structure. Nanofiber diameter decreased after drug loading. The highest average nanofiber diameter ( $282.9 \pm 64.6$  nm) was determined at the lowest drug loading ratio (0.5 wt.%). Moreover, the highest drug release ratio was reached at 0.5 wt.% drug loading (~70%). Initial burst release in first hour was less than 11% for all drug-loaded preparations.

EDS mapping was used as another characterization method for determining tetracycline hydrochloride in 0.5% drug loaded nanofiber structure. Chloride should have been searched to prove the presence of the antibiotic in copolymer/gelatin structure (Mesa et al, 2013). Results of EDS mapping confirmed that there were Cl in the structure of nanofiber. Moreover, Sulphur(S) and Nitrogen(N) peaks were determined which may have come from Gelatin in nanofiber structure (Turo et al, 2018).

SEM analysis was performed on drug loaded membranes in order to understand the changes in the structure of nanofiber after drug release experiments. SEM images showed that, at the end of the 14 days drug release, structure of copolymer/gelatin nanofibers were degraded as expected.

In this study, antibacterial activity of drug loaded copolymer/nanofiber was determined to decide the most efficient drug ratio in copolymer/gelatin membrane. Three different bacteria; *Staphylococcus aureus*, *Bacillus subtilis* as gram-positive and *Escherichia coli* as gram negative species, were selected. Disk Diffusion Method for Investigation of Antibacterial Properties of Membranes were chosen and inhibition zone of disks were calculated. Consequently, all samples with different ratios of loaded Tetracycline Hydrochloride antibiotic provided clear inhibition zones against gram-positive species. On the other hand, membranes were not enough successful against *E. coli* for 0.5% Tetracycline Hydrochloride ratio. Moreover, higher antibiotic ratio had lower activity against *E. coli*. This may be explained with, double membrane structure of *E. coli* causing resistance to the antibiotic chosen in this study (Karami et al, 2006).

In conclusion, main focus as first part of study was fabrication of biodegradable copolymer/gelatin nanofiber. As a result of the study, most efficient copolymer/gelatin nanofibers were successfully fabricated (15wt.% copolymer 8wt.% gelatin (50:50, v:v in HFIP solvent)). As the second part of the study, different amounts (0.5, 1, 3, and 5%) of tetracycline hydrochloride antibiotic were loaded to copolymer/gelatin

nanofibers and drug release behaviours of membranes were investigated. In this study, most efficient drug ratio was found as 0.5% tetracycline hydrochloride in membrane. It provided more controlled and more suitable release from membrane. Antibacterial test results showed that, 0.5% tetracycline hydrochloride ratio in membrane was not enough against *E. coli*. However, 0.5% amount of tetracycline hydrochloride loaded membrane was successful against *S. aureus*, *B. Subtilis*. According to drug release behavior, the most appropriate membrane is 0.5 wt.% drug loaded copolymer/gelatin nanofiber membrane. The antibiotic ratio of membrane can be increased to 3% for the broad spectrum effect against to bacteria.



## REFERENCES

- Al-Enizi, A., Zagho, M., & Elzatahry, A.** (2018). Polymer-Based Electrospun Nanofibers for Biomedical Applications, *Nanomaterials*, 8(4), 259. <https://doi.org/10.3390/nano8040259>
- Anu Bhushani, J., & Anandharamakrishnan, C.** (2014). Electrospinning and electrospraying techniques: Potential food based applications, *Trends in Food Science & Technology*, 38(1), 21–33. <https://doi.org/10.1016/j.tifs.2014.03.004>
- Balouiri, M., Sadiki, M., & Ibnsouda, S. K.** (2016). Methods for in vitro evaluating antimicrobial activity: A review, *Journal of Pharmaceutical Analysis*, 6(2), 71–79. <https://doi.org/10.1016/j.jpha.2015.11.005>
- Bhardwaj, N., & Kundu, S. C.** (2010a). Electrospinning: A fascinating fiber fabrication technique, *Biotechnology Advances*, 28(3), 325–347. <https://doi.org/10.1016/j.biotechadv.2010.01.004>
- Bhardwaj, N., & Kundu, S. C.** (2010b). Electrospinning: A fascinating fiber fabrication technique, *Biotechnology Advances*, 28(3), 325–347. <https://doi.org/10.1016/j.biotechadv.2010.01.004>
- Bhatarai, N., Li, Z., Gunn, J., Leung, M., Cooper, A., Edmondson, D., Veiseh, O., Chen, M.-H., Zhang, Y., Ellenbogen, R. G., & Zhang, M.** (2009). Natural-Synthetic Polyblend Nanofibers for Biomedical Applications, *Advanced Materials*, 21(27), 2792–2797. <https://doi.org/10.1002/adma.200802513>
- Bouyahyi, M., Pepels, M. P. F., Heise, A., & Duchateau, R.** (2012).  $\omega$ -Pentadecalactone Polymerization and  $\omega$ -Pentadecalactone/ $\epsilon$ -Caprolactone Copolymerization Reactions Using Organic Catalysts, *Macromolecules*, 45(8), 3356–3366. <https://doi.org/10.1021/ma3001675>
- Casper, C. L., Stephens, J. S., Tassi, N. G., Chase, D. B., & Rabolt, J. F.** (2004). Controlling Surface Morphology of Electrospun Polystyrene Fibers: Effect of Humidity and Molecular Weight in the Electrospinning Process, *Macromolecules*, 37(2), 573–578. <https://doi.org/10.1021/ma0351975>
- Cervini, P., Machado, L. C. M., Ferreira, A. P. G., Ambrozini, B., & Cavalheiro, É. T. G.** (2016). Thermal decomposition of tetracycline and chlortetracycline, *Journal of Analytical and Applied Pyrolysis*, 118, 317–324. <https://doi.org/10.1016/j.jaap.2016.02.015>
- Cervini, P., Machado, L. C. M., Ferreira, A. P. G., Ambrozini, B., & Cavalheiro, É. T. G.** (2016). Thermal decomposition of tetracycline and chlortetracycline, *Journal of Analytical and Applied Pyrolysis*, 118, 317–324. <https://doi.org/10.1016/j.jaap.2016.02.015>
- Choktaweessap, N., Arayanarakul, K., Aht-ong, D., Meechaisue, C., & Supaphol, P.** (2007). Electrospun Gelatin Fibers: Effect of Solvent System on

Morphology and Fiber Diameters, *Polymer Journal*, 39(6), 622–631.  
<https://doi.org/10.1295/polymj.PJ2006190>

- Chong, L. H., Lim, M. M., & Sultana, N.** (2015). Fabrication and Evaluation of Polycaprolactone/Gelatin-Based Electrospun Nanofibers with Antibacterial Properties, *Journal of Nanomaterials*, 2015, 1–8.  
<https://doi.org/10.1155/2015/970542>
- Domb, A. J., & Khan, W. (Eds.)**. (2014a). *Focal Controlled Drug Delivery*, Springer US. <https://doi.org/10.1007/978-1-4614-9434-8>
- Domb, A. J., & Khan, W. (Eds.)**. (2014b). *Focal Controlled Drug Delivery*, Springer US. <https://doi.org/10.1007/978-1-4614-9434-8>
- Frenot, A., & Chronakis, I. S.** (2003). Polymer nanofibers assembled by electrospinning, *Current Opinion in Colloid & Interface Science*, 8(1), 64–75. [https://doi.org/10.1016/S1359-0294\(03\)00004-9](https://doi.org/10.1016/S1359-0294(03)00004-9)
- Fu, W., Liu, Z., Feng, B., Hu, R., He, X., Wang, H., Yin, M., Huang, H., Zhang, H., & Wang, W.** (2014). Electrospun gelatin/PCL and collagen/PLCL scaffolds for vascular tissue engineering, *International Journal of Nanomedicine*, 2335. <https://doi.org/10.2147/IJN.S61375>
- Garrido-Mesa, N., Zarzuelo, A., & Gálvez, J.** (2013). Minocycline: Far beyond an antibiotic: Minocycline: far beyond an antibiotic, *British Journal of Pharmacology*, 169(2), 337–352. <https://doi.org/10.1111/bph.12139>
- Geng, X., Kwon, O., & Jang, J.** (2005). Electrospinning of chitosan dissolved in concentrated acetic acid solution, *Biomaterials*, 26(27), 5427–5432. <https://doi.org/10.1016/j.biomaterials.2005.01.066>
- Ghasemi-Mobarakeh, L., Prabhakaran, M. P., Morshed, M., Nasr-Esfahani, M.-H., & Ramakrishna, S.** (2008). Electrospun poly( $\epsilon$ -caprolactone)/gelatin nanofibrous scaffolds for nerve tissue engineering, *Biomaterials*, 29(34), 4532–4539. <https://doi.org/10.1016/j.biomaterials.2008.08.007>
- Haghi, A. K., & Akbari, M.** (2007). Trends in electrospinning of natural nanofibers, *Physica Status Solidi (a)*, 204(6), 1830–1834. <https://doi.org/10.1002/pssa.200675301>
- He, M., Jiang, H., Wang, R., Xie, Y., & Zhao, C.** (2017). Fabrication of metronidazole loaded poly ( $\epsilon$ -caprolactone)/zein core/shell nanofiber membranes via coaxial electrospinning for guided tissue regeneration, *Journal of Colloid and Interface Science*, 490, 270–278. <https://doi.org/10.1016/j.jcis.2016.11.062>
- Hu, X., Liu, S., Zhou, G., Huang, Y., Xie, Z., & Jing, X.** (2014). Electrospinning of polymeric nanofibers for drug delivery applications, *Journal of Controlled Release*, 185, 12–21. <https://doi.org/10.1016/j.jconrel.2014.04.018>
- Huang, Z.-M., Zhang, Y. Z., Ramakrishna, S., & Lim, C. T.** (2004). Electrospinning and mechanical characterization of gelatin nanofibers, *Polymer*, 45(15), 5361–5368. <https://doi.org/10.1016/j.polymer.2004.04.005>

- Huang, Z.-M., Zhang, Y.-Z., Kotaki, M., & Ramakrishna, S.** (2003). A review on polymer nanofibers by electrospinning and their applications in nanocomposites, *Composites Science and Technology*, 63(15), 2223–2253. [https://doi.org/10.1016/S0266-3538\(03\)00178-7](https://doi.org/10.1016/S0266-3538(03)00178-7)
- Ingavle, G. C., & Leach, J. K.** (2014). Advancements in Electrospinning of Polymeric Nanofibrous Scaffolds for Tissue Engineering, *Tissue Engineering Part B: Reviews*, 20(4), 277–293. <https://doi.org/10.1089/ten.teb.2013.0276>
- Jayaraman, P., Gandhimathi, C., Venugopal, J. R., Becker, D. L., Ramakrishna, S., & Srinivasan, D. K.** (2015). Controlled release of drugs in electrosprayed nanoparticles for bone tissue engineering, *Advanced Drug Delivery Reviews*, 94, 77–95. <https://doi.org/10.1016/j.addr.2015.09.007>
- Karami, N., Nowrouzian, F., Adlerberth, I., & Wold, A. E.** (2006). Tetracycline Resistance in Escherichia coli and Persistence in the Infantile Colonic Microbiota, *Antimicrobial Agents and Chemotherapy*, 50(1), 156–161. <https://doi.org/10.1128/AAC.50.1.156-161.2006>
- Karuppuswamy, P., Reddy Venugopal, J., Navaneethan, B., Luwang Laiva, A., & Ramakrishna, S.** (2015a). Polycaprolactone nanofibers for the controlled release of tetracycline hydrochloride, *Materials Letters*, 141, 180–186. <https://doi.org/10.1016/j.matlet.2014.11.044>
- Karuppuswamy, P., Reddy Venugopal, J., Navaneethan, B., Luwang Laiva, A., & Ramakrishna, S.** (2015b). Polycaprolactone nanofibers for the controlled release of tetracycline hydrochloride, *Materials Letters*, 141, 180–186. <https://doi.org/10.1016/j.matlet.2014.11.044>
- Kasapis, S., & Sablani, S. S.** (2005). A fundamental approach for the estimation of the mechanical glass transition temperature in gelatin, *International Journal of Biological Macromolecules*, 36(1–2), 71–78. <https://doi.org/10.1016/j.ijbiomac.2005.03.010>
- Katti, D. S., Robinson, K. W., Ko, F. K., & Laurencin, C. T.** (2004). Bioresorbable nanofiber-based systems for wound healing and drug delivery: Optimization of fabrication parameters, *Journal of Biomedical Materials Research*, 70B(2), 286–296. <https://doi.org/10.1002/jbm.b.30041>
- Kenawy, E., Abdel-Hay, F. I., El-Newehy, M. H., & Wnek, G. E.** (2008). processing of polymer nanofibers through electrospinning as drug delivery systems, 17.
- Ko, J. H., Yin, H., An, J., Chung, D. J., Kim, J.-H., Lee, S. B., & Pyun, D. G.** (2010). Characterization of cross-linked gelatin nanofibers through electrospinning, *Macromolecular Research*, 18(2), 137–143. <https://doi.org/10.1007/s13233-009-0103-2>
- Kundys, A., Bialecka-Florjańczyk, E., Fabiszewska, A., & Małajowicz, J.** (2018). Candida antarctica Lipase B as Catalyst for Cyclic Esters Synthesis, Their Polymerization and Degradation of Aliphatic Polyesters. *Journal of Polymers and the Environment*, 26(1), 396–407. <https://doi.org/10.1007/s10924-017-0945-1>

- Leung, V., & Ko, F.** (2011). Biomedical applications of nanofibers. *Polymers for Advanced Technologies*, 22(3), 350–365. <https://doi.org/10.1002/pat.1813>
- Li, Z., Kolb, V. M. K., Jiang, W. T., & Hong, H.** (2010). FTIR and XRD investigations of tetracycline intercalation in smectites, *Clays and Clay Minerals*, 58(4), 462–474. <https://doi.org/10.1346/CCMN.2010.0580402>
- Liu, X., & Ma, P. X.** (2009). Phase separation, pore structure, and properties of nanofibrous gelatin scaffolds, *Biomaterials*, 30(25), 4094–4103. <https://doi.org/10.1016/j.biomaterials.2009.04.024>
- Mahato, R. I.** (2007). *Pharmaceutical Dosage Forms and Drug Delivery* (1st ed.), CRC Press. <https://doi.org/10.1201/b13576>
- Matthews, J. A., Wnek, G. E., Simpson, D. G., & Bowlin, G. L.** (2002). Electrospinning of Collagen Nanofibers, *Biomacromolecules*, 3(2), 232–238. <https://doi.org/10.1021/bm015533u>
- Min, B.-M., Lee, G., Kim, S. H., Nam, Y. S., Lee, T. S., & Park, W. H.** (2004). Electrospinning of silk fibroin nanofibers and its effect on the adhesion and spreading of normal human keratinocytes and fibroblasts in vitro. *Biomaterials*, 25(7–8), 1289–1297. <https://doi.org/10.1016/j.biomaterials.2003.08.045>
- Myers, H. M., Tochon-Danguy, H. J., & Baud, C. A.** (1983). IR absorption spectrophotometric analysis of the complex formed by tetracycline and synthetic hydroxyapatite, *Calcified Tissue International*, 35(1), 745–749. <https://doi.org/10.1007/BF02405117>
- Nguyen, T.-H., & Lee, B.-T.** (2010). Fabrication and characterization of cross-linked gelatin electro-spun nano-fibers, *Journal of Biomedical Science and Engineering*, 03(12), 1117–1124. <https://doi.org/10.4236/jbise.2010.312145>
- Ohgo, K., Zhao, C., Kobayashi, M., & Asakura, T.** (2003). Preparation of non-woven nanofibers of Bombyx mori silk, Samia cynthia ricini silk and recombinant hybrid silk with electrospinning method, *Polymer*, 44(3), 841–846. [https://doi.org/10.1016/S0032-3861\(02\)00819-4](https://doi.org/10.1016/S0032-3861(02)00819-4)
- Ohkawa, K., Cha, D., Kim, H., Nishida, A., & Yamamoto, H.** (2004). Electrospinning of Chitosan, *Macromolecular Rapid Communications*, 25(18), 1600–1605. <https://doi.org/10.1002/marc.200400253>
- Pelipenko, J., Kocbek, P., & Kristl, J.** (2015). Critical attributes of nanofibers: Preparation, drug loading, and tissue regeneration, *International Journal of Pharmaceutics*, 484(1–2), 57–74. <https://doi.org/10.1016/j.ijpharm.2015.02.043>
- Ranganathan, S., Balagangadharan, K., & Selvamurugan, N.** (2019). Chitosan and gelatin-based electrospun fibers for bone tissue engineering, *International Journal of Biological Macromolecules*, 133, 354–364. <https://doi.org/10.1016/j.ijbiomac.2019.04.115>
- Rho, K. S., Jeong, L., Lee, G., Seo, B.-M., Park, Y. J., Hong, S.-D., Roh, S., Cho, J. J., Park, W. H., & Min, B.-M.** (2006). Electrospinning of collagen

nanofibers: Effects on the behavior of normal human keratinocytes and early-stage wound healing, *Biomaterials*, 27(8), 1452–1461. <https://doi.org/10.1016/j.biomaterials.2005.08.004>

*Rošic et al. - 2011—Electro-spun hydroxyethyl cellulose nanofibers th .*

**Sill, T. J., & von Recum, H. A. (2008).** Electrospinning: Applications in drug delivery and tissue engineering, *Biomaterials*, 29(13), 1989–2006. <https://doi.org/10.1016/j.biomaterials.2008.01.011>

**Soares, R. M. D., Siqueira, N. M., Prabhakaram, M. P., & Ramakrishna, S. (2018).** Electrospinning and electrospray of bio-based and natural polymers for biomaterials development, *Materials Science and Engineering: C*, 92, 969–982. <https://doi.org/10.1016/j.msec.2018.08.004>

**Supaphol, P., Suwantong, O., Sangsanoh, P., Srinivasan, S., Jayakumar, R., & Nair, S. V. (2011).** Electrospinning of Biocompatible Polymers and Their Potentials in Biomedical Applications, In R. Jayakumar & S. Nair (Eds.), *Biomedical Applications of Polymeric Nanofibers* (Vol. 246, pp. 213–239). Springer Berlin Heidelberg. [https://doi.org/10.1007/12\\_2011\\_143](https://doi.org/10.1007/12_2011_143)

**Tonda-Turo, C., Ruini, F., Ceresa, C., Gentile, P., Varela, P., Ferreira, A. M., Fracchia, L., & Ciardelli, G. (2018).** Nanostructured scaffold with biomimetic and antibacterial properties for wound healing produced by ‘green electrospinning, *Colloids and Surfaces B: Biointerfaces*, 172, 233–243. <https://doi.org/10.1016/j.colsurfb.2018.08.039>

**Ulker, C., & Guvenilir, Y. (2018a).** Enzymatic Synthesis and Characterization of Biodegradable Poly( $\omega$ -pentadecalactone-co- $\epsilon$ -caprolactone) Copolymers, *Journal of Renewable Materials*. <https://doi.org/10.7569/JRM.2017.634189>

**Ulker, C., & Guvenilir, Y. (2018b).** Enzymatic Synthesis and Characterization of Biodegradable Poly( $\omega$ -pentadecalactone-co- $\epsilon$ -caprolactone) Copolymers, *Journal of Renewable Materials*. <https://doi.org/10.7569/JRM.2017.634189>

**Van der Schueren, L., De Schoenmaker, B., Kalaoglu, Ö. I., & De Clerck, K. (2011).** An alternative solvent system for the steady state electrospinning of polycaprolactone, *European Polymer Journal*, 47(6), 1256–1263. <https://doi.org/10.1016/j.eurpolymj.2011.02.025>

**Wilberth, H. K., Manuel, C. U. J., Tania, L. C., & Manuel, A. V. (2015).** Effect of reaction temperature on the physicochemical properties of poly(pentadecanolide) obtained by enzyme-catalyzed ring-opening polymerization, *Polymer Bulletin*, 72(3), 441–452. <https://doi.org/10.1007/s00289-014-1288-x>

**Wilberth, H.-K., Manuel, C.-U. J., Tania, L.-C., & Manuel, A.-V. (2015).** Effect of reaction temperature on the physicochemical properties of poly(pentadecanolide) obtained by enzyme-catalyzed ring-opening polymerization, *Polymer Bulletin*, 72(3), 441–452. <https://doi.org/10.1007/s00289-014-1288-x>

- Xie, J., Li, X., & Xia, Y.** (2008). Putting Electrospun Nanofibers to Work for Biomedical Research: Putting Electrospun Nanofibers to Work for Biomedical Research, *Macromolecular Rapid Communications*, 29(22), 1775–1792. <https://doi.org/10.1002/marc.200800381>
- Yang, G., Xiao, Z., Long, H., Ma, K., Zhang, J., Ren, X., & Zhang, J.** (2018). Assessment of the characteristics and biocompatibility of gelatin sponge scaffolds prepared by various crosslinking methods, *Scientific Reports*, 8(1), 1616. <https://doi.org/10.1038/s41598-018-20006-y>
- Zamani, M., Morshed, M., Varshosaz, J., & Jannesari, M.** (2010). Controlled release of metronidazole benzoate from poly  $\epsilon$ -caprolactone electrospun nanofibers for periodontal diseases, *European Journal of Pharmaceutics and Biopharmaceutics*, 75(2), 179–185. <https://doi.org/10.1016/j.ejpb.2010.02.002>
- Zeng, J., Xu, X., Chen, X., Liang, Q., Bian, X., Yang, L., & Jing, X.** (2003). Biodegradable electrospun fibers for drug delivery, *Journal of Controlled Release*, 92(3), 227–231. [https://doi.org/10.1016/S0168-3659\(03\)00372-9](https://doi.org/10.1016/S0168-3659(03)00372-9)
- Zhan, J., Morsi, Y., Ei-Hamshary, H., Al-Deyab, S. S., & Mo, X.** (2016). In vitro evaluation of electrospun gelatin–glutaraldehyde nanofibers, *Frontiers of Materials Science*, 10(1), 90–100. <https://doi.org/10.1007/s11706-016-0329-9>
- Zhang, Y. Z., Venugopal, J., Huang, Z.-M., Lim, C. T., & Ramakrishna, S.** (2005). Characterization of the Surface Biocompatibility of the Electrospun PCL-Collagen Nanofibers Using Fibroblasts, *Biomacromolecules*, 6(5), 2583–2589. <https://doi.org/10.1021/bm050314k>
- Zhang, Y. Z., Venugopal, J., Huang, Z.-M., Lim, C. T., & Ramakrishna, S.** (2006). Crosslinking of the electrospun gelatin nanofibers, *Polymer*, 47(8), 2911–2917. <https://doi.org/10.1016/j.polymer.2006.02.046>
- Zong, X., Kim, K., Fang, D., Ran, S., Hsiao, B. S., & Chu, B.** (2002). Structure and process relationship of electrospun bioabsorbable nanofiber membranes, *Polymer*, 43(16), 4403–4412. [https://doi.org/10.1016/S0032-3861\(02\)00275-6](https://doi.org/10.1016/S0032-3861(02)00275-6)

## **CURRICULUM VITAE**

**Name Surname** : Ayşe Metin  
**Place and Date of Birth** : Germany-Würselen 17.11.1992  
**E-Mail** : ayse\_1662@hotmail.com

### **EDUCATION**

- **B.Sc.** : 2017, Marmara University, Faculty of Science and Art, Chemistry

### **PROFESSIONAL EXPERIENCE AND REWARDS:**

- **Macdermid Enthone-** Analitical Chemistry Intern 2014
- **Latro Chemisty-** Research and Development Specialist 2016-2017

### **OTHER PUBLICATIONS, PRESENTATIONS AND PATENTS:**

International Participation VIII. Polymer Science and Technology Congress-  
Fabrication of Nanofibers from Biopolyester/Natural Polymer Blends for Drug  
Delivery Systems- Oral Presentation-Submitted

